

This is a repository copy of *Detailed phytochemical analysis of high- and low artemisinin-producing chemotypes of Artemisia annua.*

White Rose Research Online URL for this paper:

<https://eprints.whiterose.ac.uk/130276/>

Version: Accepted Version

Article:

Czechowski, Tomasz, Larson, TR, Catania, Theresa May orcid.org/0000-0002-9882-3878 et al. (5 more authors) (2018) Detailed phytochemical analysis of high- and low artemisinin-producing chemotypes of *Artemisia annua*. *Frontiers in Plant Science*. 641. pp. 1-14. ISSN 1664-462X

<https://doi.org/10.3389/fpls.2018.00641>

Reuse

This article is distributed under the terms of the Creative Commons Attribution (CC BY) licence. This licence allows you to distribute, remix, tweak, and build upon the work, even commercially, as long as you credit the authors for the original work. More information and the full terms of the licence here:

<https://creativecommons.org/licenses/>

Takedown

If you consider content in White Rose Research Online to be in breach of UK law, please notify us by emailing eprints@whiterose.ac.uk including the URL of the record and the reason for the withdrawal request.

Detailed phytochemical analysis of high- and low artemisinin-producing chemotypes of *Artemisia annua*

Tomasz Czechowski¹, Tony R. Larson¹, Theresa Catania¹, David Harvey¹, Genxi Wei², Michel Essome², Geoffrey D. Brown^{2*}, Ian A. Graham^{1*}

¹CNAP, Department of Biology, University of York, United Kingdom, ²Department of Chemistry, University of Reading, United Kingdom

Submitted to Journal:
Frontiers in Plant Science

Specialty Section:
Plant Biotechnology

Article type:
Original Research Article

Manuscript ID:
360089

Received on:
02 Feb 2018

Revised on:
24 Apr 2018

Frontiers website link:
www.frontiersin.org

Conflict of interest statement

The authors declare that the research was conducted in the absence of any commercial or financial relationships that could be construed as a potential conflict of interest

Author contribution statement

IAG planned and supervised the experiments and wrote the manuscript.

Keywords

Artemisia annua, Chemotype, Artemisinin, NMR, Sesquiterpenes, glandular trichomes

Abstract

Word count: 248

Chemical derivatives of Artemisinin, a sesquiterpene lactone produced by *Artemisia annua*, is the active ingredient in the most effective treatment for malaria. Comprehensive phytochemical analysis of two contrasting chemotypes of *A. annua* resulted in the characterisation of over 80 natural products by NMR, more than 20 of which are novel and described here for the first time. Analysis of high- and low-artemisinin producing (HAP and LAP) chemotypes of *A. annua* confirmed the latter to have a low level of DBR2 (artemisinic aldehyde Δ^{11} (13) reductase) gene expression. Here we show that the LAP chemotype accumulates high levels of artemisinic acid, arteannuin B, epi-deoxyarteannuin B and other amorpho-4,11-diene derived sesquiterpenes which are unsaturated at the 11,13-position. By contrast, the HAP chemotype is rich in sesquiterpenes saturated at the 11,13-position (dihydroartemisinic acid, artemisinin and dihydro-epi-deoxyarteannuin B), which is consistent with higher expression levels of DBR2, and also with the presence of a HAP-chemotype version of CYP71AV1 (amorpho-4,11-diene C-12 oxidase). Our results indicate that the conversion steps from artemisinic acid to arteannuin B, epi-deoxyarteannuin B and artemisitene in the LAP chemotype are non-enzymatic and parallel the non-enzymatic conversion of DHAA to artemisinin and dihydro-epi-deoxyarteannuin B in the HAP chemotype. Interestingly, artemisinic acid in the LAP chemotype preferentially converts to arteannuin B rather than the endoperoxide bridge containing artemisitene. In contrast, in the HAP chemotype, DHAA preferentially converts to artemisinin. Broader metabolomic and transcriptomic profiling revealed significantly different terpenoid profiles and related terpenoid gene expression in these two morphologically distinct chemotypes.

Funding statement

We acknowledge financial support for this project from The Bill and Melinda Gates Foundation as well as from The Garfield Weston Foundation for the Centre for Novel Agricultural Products. This work was also supported by the Biotechnology and Biological Sciences Research Council Grant BB/G008744/1 (to GDB), "The Biosynthesis of Artemisinin".

Ethics statements

(Authors are required to state the ethical considerations of their study in the manuscript, including for cases where the study was exempt from ethical approval procedures)

Does the study presented in the manuscript involve human or animal subjects: No

1 **Detailed phytochemical analysis of high- and low artemisinin-**
2 **producing chemotypes of *Artemisia annua***

3 Tomasz Czechowski¹, Tony R. Larson¹, Theresa M. Catania¹, David Harvey¹, Cenxi Wei²,
4 Michel Essome², Geoffrey D. Brown^{2*} and Ian A. Graham^{1*}

5 ¹Centre for Novel Agricultural Products, Department of Biology, University of York,
6 Heslington, York YO10 5DD, United Kingdom

7 ²Department of Chemistry, University of Reading, Reading RG6 6AD, United Kingdom

8 *Correspondence: Geoffrey D. Brown: g.d.brown@reading.ac.uk and Ian A. Graham:
9 ian.graham@york.ac.uk

10 **Keywords: *Artemisia annua*, chemotype, artemisinin, NMR, sesquiterpenes, glandular**
11 **trichomes**

12 **Abstract**

13 Chemical derivatives of ~~a~~ Artemisinin, a sesquiterpene lactone produced by *Artemisia annua*, ~~is~~
14 are the active ingredient in the most effective treatment for malaria. Comprehensive
15 phytochemical analysis of two contrasting chemotypes of *A. annua* resulted in the
16 characterisation of over 80 natural products by NMR, more than 20 of which are novel and
17 described here for the first time. Analysis of high- and low-artemisinin producing (HAP and
18 LAP) chemotypes of *A. annua* confirmed the latter to have a low level of *DBR2* (artemisinic
19 aldehyde $\Delta^{11(13)}$ reductase) gene expression. Here we show that the LAP chemotype accumulates
20 high levels of artemisinic acid, arteannuin B, *epi*-deoxyarteannuin B and other amorpha-4,11-
21 diene derived sesquiterpenes which are unsaturated at the 11,13-position. By contrast, the HAP
22 chemotype is rich in sesquiterpenes saturated at the 11,13-position (dihydroartemisinic acid,
23 artemisinin and dihydro-*epi*-deoxyarteannunin B), which is consistent with higher expression
24 levels of *DBR2*, and also with the presence of a HAP-chemotype version of CYP71AV1
25 (amorpha-4,11-diene C-12 oxidase). Our results indicate that the conversion steps from
26 artemisinic acid to arteannuin B, *epi*-deoxyarteannuin B and artemisitene in the LAP chemotype
27 are non-enzymatic and parallel the non-enzymatic conversion of DHAA to artemisinin and
28 dihydro-*epi*-deoxyarteannuin B in the HAP chemotype. Interestingly, artemisinic acid in the LAP

29 chemotype preferentially converts to arteannuin B rather than the endoperoxide bridge
30 containing artemisitene. In contrast, in the HAP chemotype, DHAA preferentially converts to
31 artemisinin. Broader metabolomic and transcriptomic profiling revealed significantly different
32 terpenoid profiles and related terpenoid gene expression in these two morphologically distinct
33 chemotypes.

34 **1 Introduction**

35 ~~The Chemical derivatives of the~~ sesquiterpene lactone, artemisinin, ~~such as: artesunate,~~
36 ~~artemether or dihydroartemisinin~~ is-are the one of several active ingredients in artemisinin-
37 combination therapies (ACTs) - the most effective treatment for malaria currently available.
38 Biosynthesis of artemisinin occurs in specialized 10-celled biserial glandular trichomes present
39 on the leaves, stems and inflorescences of *Artemisia annua* (Duke and Paul, 1993; Duke et al.,
40 1994; Ferreira and Janick, 1995). Concentrations of artemisinin can range from 0.01% to 1.4% of
41 leaf dry weight (Larson et al., 2013). The biosynthetic pathway from artemisinin precursors has
42 been fully elucidated over the past decade (Figure 1 C). It starts from the cyclization of farnesyl
43 pyrophosphate (FPP) to amorpha-4,11-diene (A-4,11-D) by amorpha-4,11-diene synthase (AMS)
44 (Bouwmeester et al., 1999; Mercke et al., 2000) followed by the three-step oxidation of A-4,11-
45 D by amorpha-4,11-diene C-12 oxidase (CYP71AV1), to artemisinic alcohol (AAOH),
46 artemisinic aldehyde (AAA), and artemisinic acid (AA) (Ro et al., 2006; Teoh et al., 2006).
47 ADH1 – NAD-dependent alcohol dehydrogenase with specificity towards artemisinic alcohol
48 plays a role in the formation of artemisinic aldehyde in the artemisinin pathway of *A. annua*
49 (Paddon et al., 2013). The *ADH1* gene has been used to improve yields of artemisinic acid
50 production in yeast. (Paddon et al., 2013). Artemisinic aldehyde $\Delta 11(13)$ reductase (DBR2)
51 catalyzes the formation of dihydroartemisinic aldehyde (DHAAA) from AAA (Zhang et al.,
52 2008). DHAAA is subsequently oxidized in the final enzymatic reaction to dihydroartemisinic
53 acid (DHAA) by ~~alcohol-aldehyde~~ dehydrogenase ALDH1 (Teoh et al., 2009; ~~Zhang et al.,~~
54 ~~2009~~). ~~(Paddon et al., 2013)~~ Genes encoding all of these biosynthetic enzymes have been shown
55 to be highly expressed in apical and sub-apical cells of *A. annua* glandular trichomes (Olsson et
56 al., 2009; Soetaert et al., 2013). Recent studies have revealed that the conversion of DHAA to
57 artemisinin and dihydro-*epi*-deoxyarteannuin B (DHEDB) proceeds *via* a series of non-
58 enzymatic and spontaneous photochemical reactions, involving the highly reactive tertiary allylic

59 hydroperoxide of dihydroartemisinic acid, DHAAOOH (Wallaart et al., 1999; Sy and Brown,
60 2002; Brown and Sy, 2004). Similarly, it has previously been proposed that AA is
61 photochemically converted to arteannuin B (ArtB) *via* the tertiary allylic hydroperoxide of
62 artemisinic acid (Brown and Sy, 2007).

63 Based on the content of artemisinin and its precursors, two contrasting chemotypes of *A. annua*
64 have been described: a low-artemisinin production (LAP) chemotype and a high-artemisinin
65 production (HAP) chemotype (Wallaart et al., 2000). Both chemotypes contain artemisinin, but
66 the HAP chemotype has a relatively high content of DHAA and artemisinin, whereas the LAP
67 chemotype has a high content of AA and ArtB (Lomenn *et al.*, 2006; Aresenault *et al.*, 2006,
68 (Larson et al., 2013). Recent studies have concluded that a major factor in determining the
69 biochemical phenotype of HAPs and LAPs is the differential expression of *DBR2* - with low
70 expression in LAP chemotypes correlating with a number of insertions/deletions in the *DBR2*
71 promoter sequence (Yang et al., 2015). We have recently shown that the overall pathway to
72 artemisinin biosynthesis is under strict developmental control with early steps in the pathway
73 occurring in young leaves and later steps in mature leaves (Czechowski et al., 2016). In the
74 present study, we have used both metabolomics and transcriptomics to investigate the
75 developmental regulation of sesquiterpene biosynthesis in HAP and LAP chemotypes. Using a
76 combination of NMR and UPLC-/GC-MS techniques we have characterised a number of
77 amorphane and cadinane sesquiterpenes in addition to other terpenes isolated from leaf glandular
78 trichomes. We have also extended the transcript analysis in HAPs and LAPs beyond the genes
79 encoding artemisinin-pathway enzymes. Our findings suggest profound differences in general
80 terpenoid metabolism between HAP and LAP chemotypes that extend well beyond altered *DBR2*
81 expression and artemisinin content.

82 **2. Materials and methods**

83 **2.1 Plant material**

84 Artemis is an F1 hybrid variety of *A. annua* developed by Mediplant (Conthey, Switzerland),
85 produced by crossing C4 and C1 parental material of East Asian origin (Delabays et al., 2001).
86 Artemisinin content has been reported to reach 1.4% of the leaf dry weight when grown in the
87 field, and its metabolite profile is typical for the HAP chemotype (Larson *et al.*, 2013). NCV

88 (“non-commercial variety”), an “open-pollinated” variety of European origin was also provided
89 by Mediplant, and has the lowest reported artemisinin content from any *A. annua* germplasm in
90 addition to a metabolite profile characteristic of the LAP chemotype (Larson *et al.*, 2013). Plants
91 were grown from seeds in glasshouse conditions as previously described (Graham *et al.*, 2010).

92 **2.2 Leaf area measurements**

93 The leaf area of glasshouse-grown plants was measured by scanning for leaves 14-16 (counting
94 from the apical meristem), followed by calculation of the leaf area using LAMINA software
95 (Bylesjo *et al.*, 2008)

96 **2.3 Trichome density measurements**

97 Trichome density was quantified on the abaxial surface of the terminal leaflets of leaves 14-16
98 (counting from the apical meristem). Trichomes were visualised using a Zeiss fluorescent
99 dissecting microscope (fitted with a 470/40nm excitation filter/ 525/50nm emission filter).
100 Images were recorded using AxioVision 4.7 software (Carl Zeiss Ltd. Herts., UK). Trichome
101 number was counted manually across a 3 x 0.5 mm² leaflet sample area and the average (mean)
102 trichome density was then calculated for the whole leaf.

103 **2.4 NMR structural data for natural compounds from Artemis and NCV.**

104 Leaf and stem material from Artemis (5 Kg) was extracted in CHCl₃ (20 L). The organic solvent
105 was removed by rotary evaporation and a portion of the residual dark green aromatic plant
106 extract (*ca* 2.5% w/w) was “dry-loaded” on to a silica column for gradient column
107 chromatography (see Table 2.4.1).

108 **2.4.1 Gradient Column Chromatography of the Artemis variety of *A. annua***

Solvent	Fraction
10% EtOAc/hexane	A, B*, C and D*
20% EtOAc/hexane	E, F, G, H, I* and J
30% EtOAc/hexane	K, L, M, N and O*
50% EtOAc/hexane	P and Q
EtOAc	R, S, T*, U and V
Methanol	W, X and Y

109

110 Each of the fractions A-Y from gradient column chromatography of Artemis were then further
111 purified by isocratic preparative normal-phase HPLC (*fractions B, D, I, O and T were also
112 subjected to a second round of isocratic column chromatography prior to prep. HPLC); and
113 individual metabolites were then characterized by NMR, as listed in Fig. 1A and the
114 Supplemental Table 1 (1D- and 2D-NMR data for all metabolites which are novel as natural
115 products is also given in the Supplementary Section). Selected fractions were analysed by
116 UPLC-APCI-high resolution MS to verify molecular weights and chemical formulae. Confirmed
117 annotations were used to update m/z and retention time reference data, to enable reporting of
118 these compounds from plant extracts by UPLC-MS.

119 Leaf and stem material from the NCV variety of *A. annua* (780 g) was extracted in CHCl₃ (4 L).
120 The organic solvent was then removed by rotary evaporation and the residual dark green
121 aromatic plant extract (16.6 g; ca 2% w/w) was dry-loaded onto a silica column for gradient
122 column chromatography (see Table 2.4.2).

123 **2.4.2 Gradient Column Chromatography of the NCV variety of *A. annua***

Solvent	Fraction
2% EtOAc/hexane	A, B and C
10% EtOAc/hexane	D, E, F and G
20% EtOAc/hexane	G, H and I
40% EtOAc/hexane	J, K and L
EtOAc	M and N
Methanol	N

124 Each of the fractions A-N from gradient column chromatography of NCV were then further
125 purified by isocratic preparative normal-phase HPLC; individual metabolites were then
126 characterized by NMR, as listed in Fig. 1B and the Supplemental Table 1 (1D- and 2D-NMR
127 data for all metabolites which are novel as natural products are also given in the Supplementary
128 Section). Selected fractions were analysed by UPLC-APCI-high resolution MS to verify
129 molecular weights and chemical formulae. Confirmed annotations were used to update m/z and
130 retention time reference data, to enable reporting of these compounds from plant extracts by
131 UPLC-MS.

132 **2.5 Metabolite analysis by UPLC-MS and GC-MS**

133 Metabolite analysis by UPLC- and GC-MS were performed as described previously
134 (Czechowski *et al.*, 2016). Fifteen plants from each of five genotype classes were grown from
135 seeds in 4-inch pots under 16 h days for 12 weeks. Metabolite profiles were generated from 50
136 mg fresh weight (FW) pooled samples of leaves collected at two different developmental stages:
137 1-5 (counted from the apical meristem), representing the juvenile stage; and leaves 11-13,
138 representing the mature, expanded stage (Figure 1A). Fresh leaf samples were stored at -80°C,
139 pending analysis. In addition, dry leaf material was also obtained from 14-week old plants, cut
140 just above the zone of senescing leaves, and dried for 14 days at 40°C. Leaves were stripped
141 from the plants, and leaf material sieved through 5 mm mesh to remove small stems. Trichome-
142 specific metabolites were extracted as described previously (Czechowski *et al.*, 2016) with minor
143 modifications. Briefly, 50 mg of fresh material was extracted by gentle shaking in 500 µl
144 chloroform for 1 h. Supernatant was taken out and remaining plant material was fully dried in a
145 centrifugal evaporator (GeneVac® Ez-2 plus, Genevac Ltd, Ipswich, UK). Weight of the
146 extracted and dried material was taken and used to quantify abundance of the specific
147 compounds per unit of extracted dry weight. Dry leaf material (0.5 g) was ground to a fine
148 powder using a TissueLyser II ball mill fitted with stainless steel grinding jars (Qiagen, Crawley,
149 UK) operated at 25 Hz for 1 min. Ten mg sub-samples of dry leaf material were extracted in 9:1
150 (v/v) chloroform:ethanol with gentle shaking for 1 h and then analysed as per fresh material.

151 For UPLC-MS analysis of sesquiterpenes, a diluted (1:5 (v/v) extract:ethanol) 2 µL aliquot was
152 injected on an Acquity UPLC system (Waters, Elstree, UK) fitted with a Luna 50 × 2 mm 2.5 µm
153 HST column (Phenomenex, Macclesfield, UK). Metabolites were eluted at 0.6 mL/min and 60°C
154 using a linear gradient from 60% to 100% A:B over 2.5 min, where A = 5% (v/v) aqueous
155 MeOH and B = MeOH, with both A and B containing 0.1% (v/v) formic acid. Pseudomolecular
156 [M+H]⁺ ions were detected using a Thermo Fisher LTQ-Orbitrap (ThermoFisher, Hemel
157 Hempstead, UK) mass spectrometer fitted with an atmospheric pressure chemical ionization
158 source operating in positive ionisation mode under the control of Xcalibur 2.1 software. Data
159 was acquired over the m/z range 100 - 1000 in FTMS centroid mode with resolution set to 7500
160 FWHM at m/z 400. Data extraction and analysis was performed using packages and custom
161 scripts in R 3.2.2 (<https://www.R-project.org/>). XCMS (Smith *et al.*, 2006) incorporating the
162 centWave algorithm (Tautenhahn *et al.*, 2008) was used for untargeted peak extraction.
163 Deisotoping, fragment and adduct removal was performed using CAMERA (Kuhl *et al.*, 2012).

164 Artemisinin was quantified using the standard curve of the response ratio of artemisinin (Sigma,
165 Poole, UK) to internal standard (β -artemether; Hallochem Pharmaceutical, Hong Kong) that was
166 previously added to extracts and standards. Metabolites were identified with reference to
167 authentic standards or NMR-resolved structures and empirical mass formulae calculated using
168 the R package rcdk (Guha, 2007) within 10 ppm error and elemental constraints of: C = 1–100,
169 H = 1–200, O = 0–20, N = 0 – 1. Peak concentrations were calculated using bracketed response
170 curves, where standard curves were run every ~30 samples. Metabolite concentrations were
171 expressed as a proportion of the residual dry leaf material following extraction.

172 For analysis of monoterpenes and volatile sesquiterpenes from fresh leaf samples, an aliquot of
173 chloroform extract (prior to dilution with ethanol for UPLC analysis) was taken for GC-MS
174 analysis using an Agilent 6890 GC interfaced to a Leco Pegasus IV TOF MS (Leco, Stockport,
175 UK). A 1 μ L aliquot was injected into a CIS4 injector (Gerstel, Mülheim an der Ruhr, Germany)
176 fitted with a 2 mm ID glass liner containing deactivated glass wool at 10°C. The injector was
177 ramped from 10°C to 300°C at 12°C/s then held at 300°C for 5 min. The carrier gas was He at a
178 constant flow of 1 mL/min and the injection split ratio was 1:10. Peaks were eluted using a
179 Restek Rxi-5Sil MS column, 30 m x 0.25 mm ID x 0.25 μ m film thickness (Thames Restek,
180 Saunderton, UK). The following temperature gradient was used: isothermal 40°C 2 min; ramp at
181 20°C/min to 320°C then hold for 1 min; total run time ~20 min. The transfer line was
182 maintained at 250°C and the MS used to collect -70 eV EI scans over the m/z range 20–450 at a
183 scan rate of 20 spectra/second. Acquisition was controlled by ChromaTof 4.5 software (Leco).
184 ChromaTof was used to identify peaks and deconvolute spectra from each run, assuming a peak
185 width of 3 s and a minimum *s/n* of 10. Peak areas were reported as deconvoluted total ion traces
186 (DTIC). Further analyses including annotation against authentic standards, between-sample peak
187 alignment, grouping, consensus DTIC reporting, and missing value imputation were performed
188 using custom scripts in R.

189 R was used for all statistical data analysis using the stats base package, nlme ([http://CRAN.R-](http://CRAN.R-project.org/package=nlme)
190 [project.org/package=nlme](http://CRAN.R-project.org/package=nlme)) and pcaMethods (Stacklies et al., 2007)

191 **2.6 RNA isolation, cDNA synthesis and quantitative RT-PCR**

192 Leaf tissue from juvenile and mature-stage leaves sampled as described above was ground to a
193 fine powder using Qiagen Retsch MM300 TissueLyser (Qiagen, Hilden, Germany) and total
194 RNA extracted using the RNAeasy kit (Qiagen, Hilden, Germany). RNA was quantified using
195 NanoDrop-1000 (NanoDrop products, Wilmington, USA) and integrity was checked on 2200
196 Tape Station Instrument (Agilent, Santa Clara, CA, USA). Only samples scoring RIN number
197 ≥ 7.0 were taken for further analysis. Removal of genomic DNA was performed by treating with
198 TURBO DNA-free™ (Life Technologies Ltd, Paisley, UK) following manufacturer's
199 instructions. 5 ug of total RNA, pooled from 4 individual plants, representing 3 biological
200 replicates, was reversely transcribed using SuperScript II kit (Life Technologies Ltd, Paisley,
201 UK) and Oligo(dT)12-18 Primer (Life Technologies Ltd, Paisley, UK) according to
202 manufacturer's instructions. PCR using primers (AMS_Ex4 for 5'-
203 GGCTGTCTCTGCACCTCCTC-3', AMS_Ex5 for 5'- CAGCCATCAATAACGGCCTTG -3')
204 designed spanning intron 4 of the *AMS* gene (GenBank: AF327527). Only samples that resulted
205 in amplification of the 251bp fragment from cDNA and not the 363 bp fragment from genomic
206 DNA were taken for further qPCR analysis.

207 Expression levels of amorpho-4,11-diene synthase (*AMS*), amorpho-4,11-diene C-12 oxidase
208 (*CYP71AV1*), cytochrome P450 reductase (*CPR*), artemisinic aldehyde Δ 11 (13) reductase
209 (*DBR2*) and aldehyde dehydrogenase (*ALDH1*), relative to ubiquitin (*UBI*) were determined by
210 qPCR. Reactions were run in 3 technical replicates. Gene-specific primers used were: *AMS* for
211 5'- GGGAGATCAGTTTCTCATCTATGAA- 3'; *AMS_Rev* 5'-
212 CTTTTAGTAGTTGCCGCACTTCTT-3'; 5'*ALDH1* for 5'- GATGTGTGTGGCAGGGTCTC-
213 3'; *ALDH1_Rev* 5'- ACGAGTGGCGAGATCAAAAG-3'; *CYP71AV1* for 5'-
214 TCAACTGGAAACTCCCAATG-3'; *CYP71AV1_Rev* 5'- CGGTCATGTTCGATCTGGTCA-
215 3'; *CPR_For* 5'- GCTCGGAACAGCCATCTTATTCTT-3', *CPR_Rev* 5'-
216 GAAGCCTTCTGAGTCATCTTGTGT-3', *DBR2* for 5'- GAACGGACGAATATGGTGGG-3';
217 *DBR2_Rev* 5'- GCAGTATGAATTTGCAGCGGT-3', *UBI* for 5'-
218 TGATTGGCGTCGTCTTCGA-3' and *UBI_Rev* 5'-CCCATCCTCCATTTCTAGCTCAT-3'.
219 Reactions conditions and qPCR analysis were performed as above, 1 ul of 1/20 first strand cDNA
220 dilution was used instead of genomic DNA. Background subtraction, average PCR efficiency
221 for each amplicon and N_0 values were calculated using LinRegPCR ver. 2012 software (Ruijter

222 et al 2009). Expression levels for each sample and gene of interest (GOI) were represented as NO
223 GOI / NO UBI.

224 **3 Results**

225 **3.1 NMR spectroscopic analysis uncovers novel metabolites in both HAP and LAP** 226 **chemotypes**

227 The natural products found in *A. annua* have previously been grouped into eight broad
228 categories, including: i) monoterpenes; ii) sesquiterpenes; iii) diterpenes, iv) sterols and
229 triterpenes; v) aliphatic hydrocarbons, alcohols, aldehydes and acids; vi) aromatic alcohols,
230 ketones and acids; vii) phenylpropanoids; and viii) flavonoids (Brown, 2010). In the present work
231 we have used the Artemis variety of *A. annua* as a representative of the HAP chemotype and
232 NCV as a representative of the LAP chemotype (Larson et al., 2013). Our initial investigations
233 using NMR analysis of leaf extracts of Artemis resulted in the isolation of 41 metabolites (6 of
234 which were novel) representing all eight classes of natural products (Figure 1A, Supplemental
235 List 1). The structures of all compounds were determined by 1D- and 2D- NMR spectroscopy
236 (detailed NMR data in Supplementary Section). Novel compounds which have not been isolated
237 before as natural products include four new 11,13-dihydroamorphanes: 5 β -hydroperoxy-
238 eudesma-4(15),11-diene (**4**), 11-Hydroxy-arteannuin I (**18**), 6 α -Hydroxy-arteannuin J (**19**),
239 Arteannuin P (**20**); the ketal form of arteannuin Q, (**26**) and abeo-Amorphane sesquiterpene (**27**).
240 Artemisinin (**22**) was the most abundant metabolite in this analysis (Figure 2, Supplemental List
241 1, and Supplemental Table 1); but the Artemis extract also contained two other sesquiterpenes:
242 dihydroartemisinic acid (DHAA, **8**), and dihydro-*epi*-deoxyarteannuin B (DHEDB, **12**) in
243 substantial amounts (Figure 2, Supplemental List 1 and Supplemental Table 1). In addition, a
244 further nine known 11,13-dihydroamorphanes (α -epoxy-dihydroartemisinic acid (**10**); 4 α ,5 α -
245 epoxy-6 α -hydroxyamorphane-12-oic acid (**11**); dihydroarteannuin B (**14**); arteannuin M (**15**);
246 arteannuins H, I and J (**21**, **16** and **17**); deoxyartemisinin (**23**); and a 4,5-*seco*-4,5-diketo-
247 amorphane-12-oic acid (**24**) (see Figure 1A, Supplemental Figure 1 and Supplemental Table 1)
248 were also isolated as minor components from the Artemis leaf extracts (Figure 2, Supplemental
249 List 1 and Supplemental Table 1)

250 Phytochemical investigation of the NCV variety by NMR yielded 57 metabolites, 20 of which
251 were novel (Figure 1B Supplemental List 2), representing 7 of the 8 categories above. Novel
252 metabolites from NCV variety are depicted on Figure 1B and include: (*E*)-7-Hydroxy-2,7-
253 dimethylocta-2,5-dien-4-one (**43**), (*E*)-7-Hydroperoxy-2,7-dimethylocta-2,5-dien-4-on (**44**), 6,7-
254 Epoxy-6,7-dihydro- β -farnesene (**45**), 6-Hydroxy- γ -humulene (**48**), 7 α -Hydroxy-artemisinic acid
255 (**52**), Arteannuin R (**54**), Arteannuin S (**55**), 4 α , 5 α -Epoxy-6 α -hydroxyartemisinic acid methyl
256 ester (**57**), Dehydroarteannuin L (**59**), *epi*-11-Hydroxy-arteannuin I (**64**), Artemisinic acid, 6 α -
257 peroxy ester (**65**), Deoxyartemistene (**67**) (novel as a natural product¹), Arteannuin T (**69**),
258 Arteannuin U (**70**), Arteannuin V (**72**), Arteannuin W (**73**), Arteannuin Y (**74**), Isoarteannuin A
259 (**77**), Arteannuin Z (**78**) and 3-(2-(2,5-Dihydrofuran-3-yl)ethyl)-2,2-dimethyl-4-
260 methylenecyclohexan-1-one (**79**).

261 As might have been expected, the most striking difference between the NCV and *Artemis*
262 varieties was the almost complete absence of artemisinin, DHAA (**8**) and DHEDB (**12**) in the
263 former (Supplemental Table 1). The NCV variety did, however, have relatively high levels of
264 three 11-13-unsaturated amorphanes, which were found only as minor components in the
265 *Artemis* variety, namely: artemisinic acid (AA, **9**), arteannuin B (ArtB, **60**) and *epi*-
266 deoxyarteannuin B (EDB, **13**) (Figure 2, Supplemental Figure 2 and Supplemental Table 1). All
267 the other amorphane sesquiterpenes isolated and characterized from the NCV variety by NMR
268 shared this same trait: *i.e.* possession of an 11,13-unsaturated methylene group (Figure 1B,
269 Figure 2 and Supplemental Table 1), and there is an almost complete absence of 11,13-dihydro-
270 amorphanes from NCV, that contrasts with the abundance of these compounds in the *Artemis*
271 variety (Supplemental List 2 and Supplemental Table 1). It is interesting to note that there are ten
272 examples where 11,13-dihydro/ 11,13-dehydro amorphanolides seem to occur as “pairs” between
273 *Artemis* and NCV depicted on Figure 2. These include: DHAA (**8**) / AA (**9**); artemisinin (**22**) /
274 artemisitene (**65**); dihydro-*epi*-deoxyarteannuin B (**12**) / *epi*-deoxyarteannuin B (**13**); α -epoxy-
275 dihydroartemisinic acid (**10**) / α -epoxy-artemisinic acid (**56**); dihydroarteannuin B (**14**) /
276 arteannuin B (**60**); arteannuin M (**15**) / dehydroarteannuin M (**61**); arteannuin I (**16**) / annulide
277 (**62**); arteannuin J (**17**) / isoannulide (**63**); deoxyartemisinin (**23**) / deoxyartemisitene (**67**); and 4,5-
278 *seco*-4,5-diketo-amorphan-12-oic acid (**24**) and its 11,13-dehydro-analogue (**68**). It is also
279 noteworthy that 9 of the 20 novel amorphane and *seco*-amorphane sesquiterpenes isolated and
280 characterized from the NCV variety by NMR, possess an 11, 13-unsaturated methylene group
281 (Figure 1B, Supplemental List 2)

282 All the above results are consistent with a higher DBR2 activity in the HAP chemotype
283 compared to LAP chemotype (Yang *et al.*, 2015). The relative abundances for 8 of these 10
284 “pairs” are also well matched between the *Artemis* and NCV varieties, suggesting a “shared”
285 further metabolism for DHAA in *Artemis* and AA in NCV. The first exception is arteannuin B
286 (ArtB **60**), which is abundant in NCV, whilst its analogue, dihydroarteannuin B (**14**), is relatively
287 low in *Artemis*. (Supplemental Table 1). The second is artemisitene, the 11,13-dehydro analogue
288 of artemisinin (Acton *et al.*, 1985; (Woerdenbag *et al.*, 1994) (Fig 1; Supplemental Table 1)
289 which is a minor compound in NCV, while its ‘partner’ artemisinin is the most abundant
290 metabolite in *Artemis* (Supplemental Table 1). These observations suggest that while there are
291 many parallels in the pathways that further transform DHAA (**8**) and AA (**9**) in the HAP and
292 LAP chemotypes there are some significant differences.

293 **3.2 Metabolomic and gene expression studies reveal multiple differences between HAP and** 294 **LAP chemotypes.**

295 Using a leaf maturation time-series, we recently demonstrated that artemisinin levels increase
296 gradually from juvenile to mature leaves and remain stable during the post-harvest drying
297 process in *Artemis* HAP chemotype plants (Czechowski *et al.*, 2016). Using a similar time-series
298 (which included fresh leaf 1–5 (juvenile), and 11–13 (mature) (counting from the apical
299 meristem); plus oven-dried whole plant-stripped leaves (dry) from 12-week-old glasshouse-
300 grown plants), we have now performed UPLC- and GC-MS based metabolite profiling of
301 extracts from both HAP (*Artemis*) and LAP (NCV) chemotypes. We found that the pathway
302 entry-point metabolite, amorpho-4,11-diene (A-4,11-D), is only detectable in juvenile leaves,
303 and at approximately 2-fold higher concentration in *Artemis* as compared to NCV (Figure 3Ai;
304 Supplemental Table 3). A much greater difference was seen for the enzymatically-produced
305 artemisinin precursor, dihydroartemisinic acid (DHAA), which was present at a 24-fold higher
306 concentration in juvenile *Artemis* leaves compared to NCV (Figure 3A ii), Supplemental Table
307 2). Artemisinic acid (AA) on the other hand accumulated in NCV leaves at a 10-fold higher
308 concentration than in *Artemis* (Figure 3A iii), Supplemental Table 1). Interestingly the levels of
309 AA in the young leaves of NCV variety are approximately twice the levels of DHAA in young
310 leaves of *Artemis* (Figure 3A ii) and iii), Supplemental Table 2). The levels of both DHAA and
311 AA dropped sharply beyond the juvenile leaf stage in *Artemis* and NCV, respectively (Figure 3A

312 ii) and iii), Supplemental Table 2). These changes in metabolite levels occur during leaf
313 maturation are mirrored by changes in steady state mRNA levels of genes encoding the enzymes
314 involved in their biosynthesis including: amorpha-4,11-diene synthase (AMS), amorpha-4,11-
315 diene C-12 oxidase (CYP71AV1), artemisinic aldehyde $\Delta^{11,(13)}$ reductase (DBR2) and aldehyde
316 dehydrogenase (ALDH1) which are expressed at levels two to three orders of magnitude higher
317 in juvenile than in mature leaves (Figure 3B i), ii), iii), iv)).

318 Previous work has suggested that *in vivo* conversions beyond DHAA (**8**) (Czechowski *et al.*,
319 2016) and *in vitro* conversions beyond AA (**9**) (Brown and Sy, 2007) are non-enzymatic.
320 Consistent with this, we have found that mature leaves of NCV contain high levels of *epi*-
321 deoxyarteannuin B (EDB, **13**) and arteannuin B (ArtB, **60**) and (Figure 3A v) and vii),
322 Supplemental Table 2), while Artemis accumulates dihydro-*epi*-deoxyarteannuin B (DHEDB,
323 **12**) and artemisinin (**22**) (Figure 3A iv), vi) Supplemental Table 2) at 20 to 30-fold higher levels
324 than NCV. Both artemisinin (**22**) and arteannuin B (**60**) continue to accumulate in the post-
325 harvest drying process in Artemis and NCV respectively (Figure 3A vi) and vii)). Post-harvest
326 accumulation of artemisinin has been reported before (Ferreira and Luthria, 2010) and it might
327 be related to light-dependent conversion of DHAA. However slightly different batch specific
328 environmental effects during drying might explain difference between artemisinin accumulation
329 pattern shown on Figure 3A vi) and what was previously reported for the Artemis variety
330 (Czechowski *et al.*, 2016). Interestingly, the developmental pattern of DHEDB (**12**)
331 accumulation in Artemis leaves is different to its 11,13-dehydro analog, EDB (**13**) in NCV
332 leaves. DHEDB (**12**) follows the same accumulation pattern as for artemisinin (**22**) in Artemis
333 (Figure 3A iv) and vi)); whereas EDB (**13**) is found predominantly in juvenile leaves of the NCV
334 variety (Figure 3A v)). We have found that production of the artemisinin 11,13-dehydro analog,
335 artemisitene (**66**) in NCV parallels the accumulation of artemisinin (**22**) in Artemis
336 (Supplemental Table 2), albeit at very much reduced levels. The levels of deoxyartemisinin (**23**),
337 another product of non-enzymatic conversion of DHAA through the DHAA allylic
338 hydroperoxide, increase during dry leaf storage, accumulating to 0.1% leaf dry weight
339 (Supplemental Table 2), which is consistent with previous findings (Czechowski *et al.*, 2016).
340 This process is paralleled by accumulation of deoxyartemisitene (**67**) (the 11,13-dehydro analog
341 of deoxyartemisinin) in the NCV variety (Supplemental Table 2).

342 RT-qPCR analysis confirmed the expression level for *DBR2* to be significantly repressed (8-fold
343 lower) in the juvenile leaves of NCV compared to Artemis, which is consistent with previous
344 findings (Yang et al. 2015). Interestingly, *DBR2* transcript abundance had decreased to the same
345 levels in mature leaves of both chemotypes (Figure 3B iii)), highlighting the importance of
346 developmental timing in regulating flux and partitioning of sesquiterpene metabolites. More
347 surprisingly, *ALDH1* expression is increased in juvenile leaves (2.4-fold) and further increased in
348 mature leaves (40-fold) of NCV (Figure 3B iv)) compared to Artemis. Thus it would appear that
349 in addition to *DBR2* being down-regulated in the NCV (LAP) chemotype, *ALDH1* is up-
350 regulated at the transcriptional level. This could also account for the increase in flux into
351 artemisinic acid and the artemisitene branch of sesquiterpene metabolism. The major differences
352 in metabolite levels and gene expression between Artemis and NCV varieties for the artemisinin
353 biosynthetic pathway are summarized in Figure 3C.

354 NMR analysis revealed that metabolite differences between Artemis and NCV are not restricted
355 to artemisinin-related sesquiterpenes. Monoterpenes also vary between the two chemotypes, with
356 for example camphor being most abundant in Artemis while artemisia ketone level is much more
357 abundant in NCV (Supplemental Table 1). Unfortunately, NMR-analysis could only provide
358 approximate information about the relative abundance of the metabolites, therefore metabolite
359 content of both chemotypes was also studied by GC- and UPLC-MS (Supplemental Tables 2 and
360 3). We were able to detect 75 unique compounds in three leaf types by UPLC-MS of which
361 annotations were assigned to 30 compounds based on NMR-verified standards as described in
362 the Materials and Methods. The majority of the known compounds were sesquiterpenes and
363 flavonoids. GC-MS detected 202 unique compounds in juvenile and mature leaves, of which 33
364 had assigned annotations. The majority of known GC-MS-detected compounds were mono- and
365 sesquiterpenes. Using principal component analysis, it can be seen that the overall metabolite
366 profile of NCV appears strikingly different to that of Artemis; as much as the difference between
367 the profiles between juvenile leaves and mature- and/or dry leaves. In fact, UPLC- and GC-MS
368 PCA plots show four distinct clusters (Figure 4A and B). Developmental differences are most
369 apparent in juvenile leaf tissue, which show the highest abundance of most of the terpenes
370 described below (Figure 4, Supplemental Tables 2 and 3). Our findings that the metabolite
371 profiles in Artemis and NCV young leaf tissues are considerably different to mature and dry
372 leaves in both varieties are consistent with our previous findings (Czechowski et al., 2016).

373 There are a number of compounds specifically produced by NCV, mostly in low quantities
374 (Supplemental Tables 2 and 3) which have known medicinal use including, for example,
375 isofraxidin (**39**), which is five-fold more abundant in the juvenile leaves of NCV as compared to
376 Artemis (Supplemental Table 2). Isofraxidin is a coumarin with anti-inflammatory (Niu *et al.*,
377 2012) and anti-tumour activities (Yamazaki and Tokiwa, 2010). Artemisia ketone (**42**), an
378 irregular monoterpene found in the essential oil from various *A. annua* varieties displaying
379 antifungal activities (Santomauro *et al.*, 2016) is the most abundant volatile in the juvenile and
380 mature leaves of NCV, but virtually absent in Artemis (Supplemental Table 3). The juvenile and
381 mature leaves of Artemis accumulate velleral, a sesquiterpene dialdehyde which has proposed
382 antibacterial activities (Anke and Sterner, 1991), which is virtually absent in NCV variety
383 (Supplemental Table 3). GC-MS analysis further revealed that several major monoterpenes are
384 also more abundant in juvenile and mature leaves of Artemis, including camphor (3.7-fold
385 higher), camphene (3.4-fold higher), borneol, (16-fold higher), α -pinene (4.6-fold higher) and
386 1,8-cineole (8-fold higher) (Supplemental Table 3). Some minor monoterpenes detected in the
387 Artemis variety, such as: α -myrcene, α -terpinene, chrysanthenone and α -copaene, are virtually
388 absent in young and mature NCV leaves (Supplemental Table 3). A few striking differences
389 were noted for the level of artemisinin-unrelated abundant sesquiterpenes, such as sabinene and
390 *cis*-sabinene hydrate, which are 7.5-fold and 38-fold (respectively) more abundant in Artemis
391 young leaves than in NCV (Supplemental Table 3). Germacrene A is a sesquiterpene common
392 across the Asteraceae family for which it has been demonstrated that its downstream metabolism
393 parallels artemisinic acid biosynthetic pathway (Nguyen *et al.*, 2010). Germacrene A levels are
394 32- and 17-fold higher in NCV young and mature leaves (respectively) making it the most
395 abundant volatile in mature and the second most abundant in young leaves of the NCV variety.

396 Visualisation of the loadings from the multivariate analyses were used to identify the most
397 influential compounds discriminating chemotypes. PC1 loading plots identified 18 compounds
398 from UPLC- and 20 from GC-MS analysis (Supplemental Figure 1), which were used to create
399 the heatmaps presented in Figure 5. The vast majority of the most influential compounds
400 distinguishing between two chemotypes from UPLC-MS analysis were the amorphane
401 sesquiterpenes (Figure 5A). The mono- and sesquiterpenes mentioned above (together with
402 some unknown compounds) were the most influential GC-MS-detectable metabolites
403 distinguishing between two chemotypes (Figure 5B).

404 **3.3 Morphological difference between two chemotypes of *A. annua***

405 In addition to having very distinct phytochemical compositions the F1 *Artemis* HAP chemotype
406 and the open pollinated NCV LAP chemotype varieties also have very distinct morphological
407 features (Figure 6). Most strikingly, NCV is much taller with longer internodes but produces
408 smaller leaves than *Artemis*. The density of glandular secretory trichomes, the site of artemisinin
409 synthesis, is similar for both varieties (Figure 6 E), which is consistent with the main difference
410 in artemisinin production is due to an alteration in metabolism rather than trichome density. *A.*
411 *annua* varieties typically require short day length for flowering (Wetzstein et al., 2014), but we
412 observed that NCV, unlike *Artemis*, can also flower under long days. However, the two
413 chemotypes do cross-pollinate and produce viable progeny.

414 **4 Discussion**

415 This manuscript presents the first detailed phytochemical comparison of high- (HAP) and low-
416 artemisinin production (LAP) chemotypes of *A. annua*.

417 26 of the 85 metabolites that have been characterized by NMR from the HAP and LAP varieties
418 of *A. annua* in this study are novel as natural products (all are mono- and sesquiterpenes). And of
419 these, 19 are amorphane sesquiterpenes, which is the most diverse and the most abundant sub-
420 class (Supplementary Table 1, Supplementary Lists 1 and 2). The majority of these amorphane
421 sesquiterpenes are highly oxygenated with structures that would be consistent with further
422 oxidative metabolism of DHAA (11,13-saturated, **8**) in the HAP variety and AA (11,13-
423 unsaturated, **9**) in the LAP variety (Figure 1, Figure 2, Supplementary Table 1, Supplemental
424 Lists 1 and 2)

425 UPLC- and GC-MS analysis of leaf developmental series also revealed amorphanes either
426 saturated or unsaturated at the 11,13-position in the HAP and LAP chemotypes, respectively
427 (Figure 3, Supplemental Table 2). This observation is consistent with the expression of the *DBR2*
428 gene, which encodes the enzyme responsible for reducing the 11,13-double bond of artemisinic
429 aldehyde (the precursor for 11,13-dihydroamorphane/cadinane sesquiterpenes) being strongly
430 down-regulated in juvenile leaves of NCV (Figure 3B iii). These findings are in complete
431 agreement with the recent report on reduced levels of *DBR2* in LAP compared with HAP
432 chemotypes (Yang *et al.*, 2015). In addition to altered expression of *DBR2*, we also found that

433 expression of *aldehyde dehydrogenase* (*ALDH1*), which converts artemisinic and
434 dihydroartemisinic aldehydes to acids (Teoh et al., 2009), is significantly elevated in juvenile and
435 mature leaves of NCV compared to Artemis. This may lead to an increased flux from A-4,11-D
436 to AA in NCV when compared with flux from A-4,11-D to DHAA in Artemis which is reflected
437 by significantly higher concentration of AA found in juvenile leafs of NCV when compared to
438 concentration of DHAA in Artemis young leaves (Figure 3A iii) and ii). ~~could enable increased~~
439 ~~flux from artemisinic aldehyde to artemisinic acid which we have observed in young leaves of~~
440 ~~NCV variety (Figure 3B iv).~~ The elevated flux from A-4,11-D to AA might also explain lower
441 levels of A-4,11-D found in juvenile leaves of NCV when compared with Artemis (Figure 3A i)
442 as the expression of *amorpha-4,11-diene synthase* (*AMS*) is at very similar level in both varieties
443 (Figure 3B i). We have also observed that the NCV (LAP) variety expresses a sequence variant
444 of *amorpha-4,11-diene C-12 oxidase* (*CYP71AV1*) with a 7 amino acid N-extension
445 (Supplemental Figure 2). This LAP-chemotype associated is sequence ~~variant was previously~~
446 ~~shown variant upon transient expression in *Nicotiana benthamiana*, in combination with the~~
447 ~~other artemisinin pathway genes resulted (Ting et al., 2013a)in a qualitatively different product~~
448 ~~profile ('chemotype'); that is ,in a shift in the ratio between the unsaturated and saturated~~
449 ~~(dihydro) branch of the pathway (Ting et al., 2013a).~~ That result strongly suggests the two
450 distinct isoforms of *CYP71AV1* are associated with HAP- and LAP-branches of the artemisinin
451 pathway also in *Artemisia annua* (Figure 3 C). ~~to be more efficient in the conversion of amorpha-~~
452 ~~4,11-diene to artemisinic acid (AA) than to artemisinic aldehyde (AAA) (Ting et al., 2013b).~~
453 ~~Thus in NCV we find decreased expression of *DBR2*, increased expression of *ALDH1* and the~~
454 ~~presence of a sequence variant of *CYP71AV1* that favours conversion of AAA to AA. We~~
455 ~~propose that these factors (Ting et al., 2013a)together lead to an increased flux from A 4,11 D to~~
456 ~~AA in NCV when compared with flux from A 4,11 D to DHAA in Artemis which is reflected by~~
457 ~~significantly higher concentration of AA found in juvenile leafs of NCV when compared to~~
458 ~~concentration of DHAA in Artemis young leaves (Figure 3A iii) and ii).~~ The elevated flux from
459 A 4,11 D to AA might also explain lower levels of A 4,11 D found in juvenile leaves of NCV
460 when compared with Artemis (Figure 3A i) as the expression of *amorpha 4,11 diene synthase*
461 (*AMS*) is at very similar level in both varieties (Figure 3B i). A number of previous reports
462 described the existence of LAP- and HAP-chemotypes of *A. annua* arising from distinct
463 geographical locations (Lommen et al., 2006); (Arsenault et al., 2010), (Larson et al., 2013). It

464 would be interesting to establish if sequence variant forms of *CYP71AV1* and differential
465 expression of *DBR2* are generally found between these other LAP- and HAP-chemotypes.

466 Recent attempts to constitutively overexpress *DBR2* in transgenic *A. annua* resulted in doubling
467 of the artemisinin concentration, which was also accompanied by a significant increase in DHAA
468 and AA production (Yuan et al., 2015). Improvements in artemisinin concentration obtained in
469 these experiments by Yuan *et al.* were significantly better than those achieved by constitutive co-
470 expression of *CYP71AV1* and *CPR* (Shen et al., 2012), where the LAP-sequence variant of
471 *CYP71AV1* was overexpressed in transgenic *A. annua*. Our results suggest the glandular
472 trichome-targeted overexpression of *DBR2* specifically in the HAP-type of *CYP71AV1* might be
473 the more efficient route to improving artemisinin production in transgenic *A. annua*

474 Although arteannuin B (ArtB) was almost entirely absent from young leaf tissue of the NCV
475 variety, as leaves matured it accumulated to become the most abundant natural product (Figure
476 3A vii). This first observation seemed to parallel both the accumulation of artemisinin in the
477 mature tissues of Artemis that has been noted above (Figure 3vi), as well as the recently
478 described accumulation of arteannuin X in the mature leaves of the *cyp71av1-1* mutant of *A.*
479 *annua* (Czechowski et al., 2016). The accumulation of both artemisinin and arteannuin X are
480 considered to be the result of non-enzymatic processes, in which the 4,5-double bond of a
481 precursor sesquiterpene undergoes spontaneous autoxidation with molecular oxygen to produce a
482 tertiary allylic hydroperoxide. The metabolic fate of this hydroperoxide is critically dependant on
483 the identity of the precursor – and in particular on the functionality contained elsewhere in the
484 molecule. Thus, in the case of Artemis, the precursor is DHAA which presents a 12-carboxylic
485 acid group (as well as saturation at the 11,13-position); whilst for the *cyp71av1-1* mutant it is
486 amorpha-4,11-diene (A-4,11-D), which presents a 11,13-double bond (Czechowski et al., 2016).
487 Both *in vivo* and *in vitro* experiments indicate that this difference in functionality is the basis
488 why DHAA-OOH (the tertiary allylic hydroperoxide from DHAA) is converted to artemisinin,
489 whereas A-4,11-D-OOH is converted to arteannuin X (Czechowski et al., 2016).

490 We therefore hypothesised that the conversion of artemisinic acid (AA) to artemisitene (Art B) in
491 NCV may also be a non-enzymatic process, paralleling the conversion of DHAA into artemisinin
492 in Artemis (Supplemental figure 3A and B) and of amorpha-4,11-diene to arteannuin X in the
493 *cyp71av1-1* mutant (Czechowski et al., 2016). The tertiary allylic hydroperoxide from

494 artemisinic acid (AA-OOH) differs from the two foregoing examples in that it incorporates both
495 a 12-carboxylic acid group and unsaturation at the 11,13-position. In support of this hypothesis,
496 when a sample of AA-OOH (produced by photosensitized oxygenation of AA; and purified by
497 HPLC) was left unattended for several weeks, it was indeed found to have been converted
498 predominantly to ArtB (albeit at a rate that was significantly slower than for the conversion of
499 DHAA-OOH to artemisinin). This unexpected transformation is mostly simply explained by
500 attack of the 12-carboxylic acid group at the allylic position of the hydroperoxide, as is shown in
501 Supplemental figure 3A and B. Further studies will be required to explain why it should be that
502 this (apparently) rather subtle modification to the 12-CO₂H group (i.e. the introduction of 11,13-
503 unsaturation in AA-OOH) has resulted in such a radically different pathway, as compared with
504 DHAA-OOH.

505 The second most abundant product of AA-OOH conversion is *Epi*-deoxyarteannuin B (EDB),
506 which accumulates predominantly in young leaves of NCV. The EDB accumulation pattern is
507 therefore different to DHEDB (the 11,13-saturated analogue), where the latter's concentration
508 rises from top to mature and dry leaves in *Artemis*, broadly following the accumulation pattern
509 of artemisinin. We have proposed that the spontaneous conversions of AA into EDB and DHAA
510 into DHEDB progress via very similar molecular mechanisms (Supplemental figure 3C and D).
511 Interestingly we have observed very little EDB arising from the spontaneous conversions of AA-
512 OOH described above, which was predominantly converted to ArtB. It is known that a
513 hydrophobic (lipophilic) environment promotes conversions of DHAA-OOH into artemisinin
514 whereas an aqueous, acidic medium promotes DHAA-OOH conversions to DHEDB (Brown and
515 Sy, 2004). This may also explain the very minor conversion of AA-OOH into EDB which was
516 carried out in a hydrophobic environment (deuterated chloroform), and which promoted AA-
517 OOH conversions to ArtB. This highlights the parallels between artemisinin and arteannuin B
518 biogenesis shown in Supplemental figure 3A and B. It also suggests that *in vivo* conversions of
519 AA-OOH to EDB requires an aqueous intra-cellular environment, which might be expected to be
520 present in young leaf trichomes, but less so in mature leaf trichomes where the sub-apical
521 hydrophobic cavities are predominant (Ferreira and Janick, 1995), or upon cell dehydration (in
522 dried leaf material).

523 Differences between the LAP and HAP chemotypes extended well beyond artemisinin-related
524 sesquiterpenes to other classes of terpenes (Figure 4, 5, Supplemental Tables 1, 2 and 3). This
525 divergence at the level of metabolism is not that surprising given that these chemotypes also
526 exhibit significant differences in their morphology (Figure 5). Artemis is an F1 hybrid derived
527 from HAP parents of East Asian origin (Delabays et al., 2001) while NCV is an open-pollinated
528 variety of Europe origin (personal communication with Dr. Michael Schwerdtfeger, curator of
529 Botanical Garden at the University of Göttingen, Germany). This is consistent with the general
530 trend for the *A. annua* varieties of European and North American which mostly represent the
531 LAP chemotype and the majority of East-Asian origin varieties which represent the HAP
532 chemotype (Wallart *et al.*, 2000), Details of the genetic divergence of these varieties remains a
533 topic for further investigation that could reveal further insight into the sesquiterpene flux into
534 different end products.

535 **5 Conclusion**

536 This first comparative phytochemical analysis of high- (HAP) and low-artemisinin production
537 (LAP) chemotypes of *A. annua* resulted in the characterisation of over 84 natural products by
538 NMR, 26 of which have not previously been described in *A. annua*. We have also shown that the
539 vast majority of *amorphane* sesquiterpenes are unsaturated at the 11,13-position in LAP-
540 chemotype as opposed to the majority of them being saturated at the 11,13-position in HAP-
541 chemotype. This is explained by existence of two sequence variants of *CYP71AV1* in the two
542 investigated chemotypes and differential expression of the key branching enzyme in artemisinin
543 pathway, namely *artemisinic aldehyde Δ 11 (13) reductase (DBR2)*. By highlighting the main
544 points of difference between HAP and LAP chemotypes our findings will help inform strategies
545 for the future improvement of artemisinin production in either *A. annua* or heterologous hosts.

546 **6 Author Contributions**

547 TC planned and performed the experiments, analysed the data, and wrote the manuscript. TRL
548 planned the UPLC-MS and GC-MS experiments, analysed data and reviewed the manuscript.
549 TMC planned and performed morphological plant analysis. DH performed UPLC-MS and GC-
550 MS experiments. CW planned and performed extraction, purifications and NMR experiments
551 and analysed data. ME performed extraction, purifications and NMR experiments. GDB planned

552 and performed NMR experiments, analysed data, wrote and reviewed manuscript. IAG planned
553 and supervised the experiments and wrote the manuscript.

554 **7 Funding**

555 We acknowledge financial support for this project from The Bill and Melinda Gates Foundation
556 as well as from The Garfield Weston Foundation for the Centre for Novel Agricultural Products
557 This work was also supported by the Biotechnology and Biological Sciences Research Council
558 Grant BB/G008744/1 (to GDB), “The Biosynthesis of Artemisinin”.

559 **8 Conflict of Interest Statement**

560 All authors declare that the research was conducted in the absence of any commercial or
561 financial relationships that could be construed as a potential conflict of interest.

562 **9 Acknowledgements**

563 We would like to thank: Dr Caroline Calvert for project management; C. Abbot and A. Fenwick
564 for horticulture assistance; X. Simonnet and Médiplant for access to the Artemis and NCV
565 varieties. We acknowledge financial support for this project from The Bill and Melinda Gates
566 Foundation. GDB would like to thank the BBSRC for financial support and the Chemical
567 Analysis Facility (CAF) at the University of Reading for the provision of the 700 MHz NMR
568 spectrometer used in these studies.

569 **10 References**

- 570 Acton, N.; Klayman, D.L. (1985) Artemisitene, a new sesquiterpene lactone endoperoxide from
571 *Artemisia annua*. 441-442.
- 572 Anke, H., and Sterner, O. (1991). Comparison of the Antimicrobial and Cytotoxic Activities of Twenty
573 Unsaturated Sesquiterpene Dialdehydes from Plants and Mushrooms. *Planta Med* 57(04), 344-
574 346. doi: 10.1055/s-2006-960114.
- 575 Arsenault, P.R., Vail, D., Wobbe, K.K., Erickson, K., and Weathers, P.J. (2010). Reproductive development
576 modulates gene expression and metabolite levels with possible feedback inhibition of
577 artemisinin in *Artemisia annua*. *Plant Physiol* 154(2), 958-968. doi: 10.1104/pp.110.162552.
- 578 Bouwmeester, H.J., Wallaart, T.E., Janssen, M.H.A., van Loo, B., Jansen, B.J.M., Posthumus, M.A., et al.
579 (1999). Amorpha-4,11-diene synthase catalyses the first probable step in artemisinin
580 biosynthesis. *Phytochemistry* 52(5), 843-854. doi: Doi 10.1016/S0031-9422(99)00206-X.
- 581 Brown, G.D. (2010). The biosynthesis of artemisinin (Qinghaosu) and the phytochemistry of *Artemisia*
582 *annua* L. (Qinghao). *Molecules* 15(11), 7603-7698. doi: 10.3390/molecules15117603.

583 Brown, G.D., and Sy, L.-K. (2004). In vivo transformations of dihydroartemisinic acid in *Artemisia annua*
584 plants. *Tetrahedron* 60(5), 1139-1159. doi: 10.1016/j.tet.2003.11.070.

585 Brown, G.D., and Sy, L.-K. (2007). In vivo transformations of artemisinic acid in *Artemisia annua* plants.
586 *Tetrahedron* 63(38), 9548-9566. doi: 10.1016/j.tet.2007.06.062.

587 Bylesjo, M., Segura, V., Soolanayakanahally, R.Y., Rae, A.M., Trygg, J., Gustafsson, P., et al. (2008).
588 LAMINA: a tool for rapid quantification of leaf size and shape parameters. *BMC Plant Biol* 8, 82.
589 doi: 10.1186/1471-2229-8-82.

590 Czechowski, T., Larson, T.R., Catania, T.M., Harvey, D., Brown, G.D., and Graham, I.A. (2016). *Artemisia*
591 *annua* mutant impaired in artemisinin synthesis demonstrates importance of nonenzymatic
592 conversion in terpenoid metabolism. *Proc Natl Acad Sci U S A* 113(52), 15150-15155. doi:
593 10.1073/pnas.1611567113.

594 Delabays, N., Simonnet, X., and Gaudin, M. (2001). The genetics of artemisinin content in *Artemisia*
595 *annua* L. and the breeding of high yielding cultivars. *Curr Med Chem* 8(15), 1795-1801.

596 Duke, M.V., Paul, R.N., Elsohly, H.N., Sturtz, G., and Duke, S.O. (1994). Localization of Artemisinin and
597 Artemisitene in Foliar Tissues of Glanded and Glandless Biotypes of *Artemisia-Annua* L.
598 *International Journal of Plant Sciences* 155(3), 365-372. doi: Doi 10.1086/297173.

599 Duke, S.O., and Paul, R.N. (1993). Development and Fine Structure of the Glandular Trichomes of
600 *Artemisia annua* L. *International Journal of Plant Sciences* 154(1), 107-118. doi:
601 10.2307/2995610.

602 Ferreira, J.F., and Luthria, D.L. (2010). Drying affects artemisinin, dihydroartemisinic acid, artemisinic
603 acid, and the antioxidant capacity of *Artemisia annua* L. leaves. *J Agric Food Chem* 58(3), 1691-
604 1698. doi: 10.1021/jf903222j.

605 Ferreira, J.F.S., and Janick, J. (1995). Floral Morphology of *Artemisia-Annua* with Special Reference to
606 Trichomes. *International Journal of Plant Sciences* 156(6), 807-815. doi: Doi 10.1086/297304.

607 Graham, I.A., Besser, K., Blumer, S., Branigan, C.A., Czechowski, T., Elias, L., et al. (2010). The genetic
608 map of *Artemisia annua* L. identifies loci affecting yield of the antimalarial drug artemisinin.
609 *Science* 327(5963), 328-331. doi: 10.1126/science.1182612.

610 Guha, R. (2007). Chemical Informatics Functionality in R. *2007* 18(5), 16. doi: 10.18637/jss.v018.i05.

611 Kuhl, C., Tautenhahn, R., Bottcher, C., Larson, T.R., and Neumann, S. (2012). CAMERA: an integrated
612 strategy for compound spectra extraction and annotation of liquid chromatography/mass
613 spectrometry data sets. *Anal Chem* 84(1), 283-289. doi: 10.1021/ac202450g.

614 Larson, T.R., Branigan, C., Harvey, D., Penfield, T., Bowles, D., and Graham, I.A. (2013). A survey of
615 artemisinic and dihydroartemisinic acid contents in glasshouse and global field-grown
616 populations of the artemisinin-producing plant *Artemisia annua* L. *Industrial Crops and Products*
617 45, 1-6. doi: 10.1016/j.indcrop.2012.12.004.

618 Lommen, W.J.M., Schenk, E., Bouwmeester, H.J., and Verstappen, F.W.A. (2006). Trichome dynamics
619 and artemisinin accumulation during development and senescence of *Artemisia annua* leaves.
620 *Planta Medica* 72(4), 336-345. doi: 10.1055/s-2005-916202.

621 Mercke, P., Bengtsson, M., Bouwmeester, H.J., Posthumus, M.A., and Brodelius, P.E. (2000). Molecular
622 cloning, expression, and characterization of amorpho-4,11-diene synthase, a key enzyme of
623 artemisinin biosynthesis in *Artemisia annua* L. *Arch Biochem Biophys* 381(2), 173-180. doi:
624 10.1006/abbi.2000.1962.

625 Nguyen, D.T., Gopfert, J.C., Ikezawa, N., Macnevin, G., Kathiresan, M., Conrad, J., et al. (2010).
626 Biochemical conservation and evolution of germacrene A oxidase in asteraceae. *J Biol Chem*
627 285(22), 16588-16598. doi: 10.1074/jbc.M110.111757.

628 Niu, X., Xing, W., Li, W., Fan, T., Hu, H., and Li, Y. (2012). Isofraxidin exhibited anti-inflammatory effects
629 in vivo and inhibited TNF-alpha production in LPS-induced mouse peritoneal macrophages in

630 vitro via the MAPK pathway. *Int Immunopharmacol* 14(2), 164-171. doi:
631 10.1016/j.intimp.2012.06.022.

632 Olsson, M.E., Olofsson, L.M., Lindahl, A.L., Lundgren, A., Brodelius, M., and Brodelius, P.E. (2009).
633 Localization of enzymes of artemisinin biosynthesis to the apical cells of glandular secretory
634 trichomes of *Artemisia annua* L. *Phytochemistry* 70(9), 1123-1128. doi:
635 10.1016/j.phytochem.2009.07.009.

636 Paddon, C.J., Westfall, P.J., Pitera, D.J., Benjamin, K., Fisher, K., McPhee, D., et al. (2013). High-level
637 semi-synthetic production of the potent antimalarial artemisinin. *Nature* 496(7446), 528-532.
638 doi: 10.1038/nature12051.

639 Ro, D.K., Paradise, E.M., Ouellet, M., Fisher, K.J., Newman, K.L., Ndungu, J.M., et al. (2006). Production of
640 the antimalarial drug precursor artemisinic acid in engineered yeast. *Nature* 440(7086), 940-943.
641 doi: 10.1038/nature04640.

642 Santomauro, F., Donato, R., Sacco, C., Pini, G., Flamini, G., and Bilia, A.R. (2016). Vapour and Liquid-
643 Phase *Artemisia annua* Essential Oil Activities against Several Clinical Strains of *Candida*. *Planta*
644 *Med* 82(11/12), 1016-1020. doi: 10.1055/s-0042-108740.

645 Shen, Q., Chen, Y.F., Wang, T., Wu, S.Y., Lu, X., Zhang, L., et al. (2012). Overexpression of the cytochrome
646 P450 monooxygenase (*cyp71av1*) and cytochrome P450 reductase (*cpr*) genes increased
647 artemisinin content in *Artemisia annua* (Asteraceae). *Genet Mol Res* 11(3), 3298-3309. doi:
648 10.4238/2012.September.12.13.

649 Smith, C.A., Want, E.J., O'Maille, G., Abagyan, R., and Siuzdak, G. (2006). XCMS: processing mass
650 spectrometry data for metabolite profiling using nonlinear peak alignment, matching, and
651 identification. *Anal Chem* 78(3), 779-787. doi: 10.1021/ac051437y.

652 Soetaert, S.S., Van Neste, C.M., Vandewoestyne, M.L., Head, S.R., Goossens, A., Van Nieuwerburgh, F.C.,
653 et al. (2013). Differential transcriptome analysis of glandular and filamentous trichomes in
654 *Artemisia annua*. *BMC Plant Biol* 13, 220. doi: 10.1186/1471-2229-13-220.

655 Stacklies, W., Redestig, H., Scholz, M., Walther, D., and Selbig, J. (2007). *pcaMethods*--a bioconductor
656 package providing PCA methods for incomplete data. *Bioinformatics* 23(9), 1164-1167. doi:
657 10.1093/bioinformatics/btm069.

658 Sy, L.K., and Brown, G.D. (2002). The role of the 12-carboxyllic acid group in the spontaneous
659 autoxidation of dihydroartemisinic acid. *Tetrahedron* 58(5), 909-923. doi: Doi 10.1016/S0040-
660 4020(01)01192-9.

661 Tautenhahn, R., Bottcher, C., and Neumann, S. (2008). Highly sensitive feature detection for high
662 resolution LC/MS. *BMC Bioinformatics* 9, 504. doi: 10.1186/1471-2105-9-504.

663 Teoh, K.H., Polichuk, D.R., Reed, D.W., and Covello, P.S. (2009). Molecular cloning of an aldehyde
664 dehydrogenase implicated in artemisinin biosynthesis in *Artemisia annua*
665 *Botany* 87(6), 635-642. doi: 10.1139/b09-032.

666 Teoh, K.H., Polichuk, D.R., Reed, D.W., Nowak, G., and Covello, P.S. (2006). *Artemisia annua* L.
667 (Asteraceae) trichome-specific cDNAs reveal CYP71AV1, a cytochrome P450 with a key role in
668 the biosynthesis of the antimalarial sesquiterpene lactone artemisinin. *FEBS Lett* 580(5), 1411-
669 1416. doi: 10.1016/j.febslet.2006.01.065.

670 Ting, H.M., Wang, B., Ryden, A.M., Woittiez, L., van Herpen, T., Verstappen, F.W., et al. (2013a). The
671 metabolite chemotype of *Nicotiana benthamiana* transiently expressing artemisinin biosynthetic
672 pathway genes is a function of CYP71AV1 type and relative gene dosage. *New Phytol* 199(2),
673 352-366. doi: 10.1111/nph.12274.

674 Ting, H.M., Wang, B., Ryden, A.M., Woittiez, L., van Herpen, T., Verstappen, F.W.A., et al. (2013b). The
675 metabolite chemotype of *Nicotiana benthamiana* transiently expressing artemisinin biosynthetic

676 pathway genes is a function of CYP71AV1 type and relative gene dosage. *New Phytologist*
677 199(2), 352-366. doi: 10.1111/nph.12274.

678 Wallaart, T.E., Pras, N., Beekman, A.C., and Quax, W.J. (2000). Seasonal variation of artemisinin and its
679 biosynthetic precursors in plants of *Artemisia annua* of different geographical origin: Proof for
680 the existence of chemotypes. *Planta Medica* 66(1), 57-62. doi: Doi 10.1055/S-2000-11115.

681 Wallaart, T.E., Pras, N., and Quax, W.J. (1999). Isolation and identification of dihydroartemisinic acid
682 hydroperoxide from *Artemisia annua*: A novel biosynthetic precursor of artemisinin. *Journal of*
683 *Natural Products* 62(8), 1160-1162. doi: Doi 10.1021/Np9900122.

684 Wetzstein, H.Y., Porter, J.A., Janick, J., and Ferreira, J.F. (2014). Flower morphology and floral sequence
685 in *Artemisia annua* (Asteraceae)1. *Am J Bot* 101(5), 875-885. doi: 10.3732/ajb.1300329.

686 Woerdenbag, H.J., Pras, N., Chan, N.G., Bang, B.T., Bos, R., Vanuden, W., et al. (1994). Artemisinin,
687 Related Sesquiterpenes, and Essential Oil in *Artemisia-Annua* during a Vegetation Period in
688 Vietnam. *Planta Medica* 60(3), 272-275. doi: DOI 10.1055/s-2006-959474.

689 Yamazaki, T., and Tokiwa, T. (2010). Isofraxidin, a coumarin component from *Acanthopanax senticosus*,
690 inhibits matrix metalloproteinase-7 expression and cell invasion of human hepatoma cells. *Biol*
691 *Pharm Bull* 33(10), 1716-1722.

692 Yang, K., Monafared, R.S., Wang, H., Lundgren, A., and Brodelius, P.E. (2015). The activity of the
693 artemisinic aldehyde Delta11(13) reductase promoter is important for artemisinin yield in
694 different chemotypes of *Artemisia annua* L. *Plant Mol Biol*. doi: 10.1007/s11103-015-0284-3.

695 Yuan, Y., Liu, W.H., Zhang, Q.Z., Xiang, L.E., Liu, X.Q., Chen, M., et al. (2015). Overexpression of
696 artemisinic aldehyde Delta 11 (13) reductase gene-enhanced artemisinin and its relative
697 metabolite biosynthesis in transgenic *Artemisia annua* L. *Biotechnology and Applied*
698 *Biochemistry* 62(1), 17-23. doi: 10.1002/bab.1234.

699 ~~Zhang, Y., Teoh, K.H., Reed, D.W., and Covello, P.S. (2009). Molecular cloning and characterization of~~
700 ~~Dbr1, a 2-alkenal reductase from *Artemisia annua* The nucleotide sequence reported in this~~
701 ~~article has been deposited in the GenBank database under accession No. FJ750460. This paper is~~
702 ~~one of a selection of papers published in a Special Issue from the National Research Council of~~
703 ~~Canada—Plant Biotechnology Institute. *Botany* 87(6), 643-649. doi: 10.1139/b09-033.~~

704 Zhang, Y., Teoh, K.H., Reed, D.W., Maes, L., Goossens, A., Olson, D.J., et al. (2008). The molecular cloning
705 of artemisinic aldehyde Delta11(13) reductase and its role in glandular trichome-dependent
706 biosynthesis of artemisinin in *Artemisia annua*. *J Biol Chem* 283(31), 21501-21508. doi:
707 10.1074/jbc.M803090200.

708

709 **Figure legends:**

710 **Figure 1. Novel natural compounds characterised from the Artemis (A) and NCV (B)**
711 **varieties of *A. annua* by NMR approach.**

712 Numbering of compounds is consistent with Supplemental Lists 1 and 2. Numbering of carbon
713 atoms showed.

714 **Figure 2. Ten pairs of 11,13-dihydro/ 11,13-dehydro amorphanolides between Artemis**
715 **(left-hand side) and NCV (right-hand side) varieties of *A. annua* characterised by the NMR**
716 **approach.**

717 Numbering of compounds is consistent with Supplemental Lists 1 and 2. Numbering of carbon
718 atoms showed. Novel compound indicated by asterisk

719 **Figure 3. Metabolic and transcriptomic comparison of the artemisinin pathway in the low-**
720 **versus high-artemisinin chemotypes of *A. annua***

721 **(A)** Level of selected sesquiterpenes were quantified by GC-MS **(i)** and UPLC-MS **(ii)-(vii)** in
722 fresh juvenile leaf 1-5 (Top), fresh mature leaf 11-13 (Mid.) and oven-dried whole plant-stripped
723 leaves (Dry) from 12-weeks old glasshouse-grown Artemis (green bars) and NCV (grey bars)
724 varieties as described in [Materials and methods. SI](#); error bars – SEM (n=15 for Top and Mid.
725 leaf; n=6 for Dry leaf). Letters represent Tukey's range test results after one way ANOVA or
726 REML (see Materials and Methods for details). Groups not sharing letters indicate statistically
727 significant differences. **(B)** – Transcript profiling of enzymes involved in the artemisinin
728 biosynthetic pathway, in two types of leaf material as on panel (A) was done as described in
729 materials and methods, error bars – SE (n=9). Asterisk indicates t-test statically significant
730 difference between Artemis (green bars) and NCV (grey bars) at p<0.05. **(C)** Summary of the
731 metabolite and transcriptional differences between Artemis and NCV for the artemisinin
732 biosynthetic pathway: full arrows – known enzymatic steps, dashed arrows – non-enzymatic
733 conversions, red arrows – transcript changes in juvenile leaves of NCV vs. Artemis, green
734 arrows – metabolite changes of NCV vs. Artemis (all types of leaves). DBR2 position in the
735 pathway highlighted in a square.

736 Metabolite abbreviations: G-3-P – glyceraldehyde-3-phosphate; MEP - 2-C-methylerythritol 4-
737 phosphate; MEcPP - 2-C-methyl-D-erythritol-2,4-cyclopyrophosphate. Cytosolic precursors:
738 HMG-CoA - 3-hydroxy-3-methylglutaryl-CoA; MVA – mevalonate; IPP – isopentenyl
739 pyrophosphate; DMAPP – dimethylallyl pyrophosphate; FPP – farnesyl pyrophosphate; A-4,11-
740 D – amorpha-4,11-diene; AAOH – artemsinic alcohol; AAA – artemsinic aldehyde; AA –
741 artemsinic acid; ArtB – arteannuin B; DHAAA - dihydroartemisinic aldehyde; DHAA -
742 dihydroartemisinic acid; DHAAOOH- dihydroartemisinic acid tertiary hydroperoxide; DHEDB –
743 dihydro-*epi*-deoxyarteannuin B. AAOOH - artemsinic acid tertiary hydroperoxide, EDB – *epi*-
744 deoxyarteannuin B. Enzyme abbreviations: HMGR- 3-hydroxy-3-methylglutaryl coenzyme A
745 reductase, HDR- 4-hydroxy-3-methylbut-2-enyl diphosphate reductase, DXR - 1-deoxy-D-
746 xylulose-5-phosphate reductoisomerase, DXS- 1-deoxy-D-xylulose-5-phosphate synthase, FPS -
747 farnesyl diphosphate synthase. AMS – amorpha-4,11-diene synthase, CYP71AV1 - amorpha-
748 4,11-diene C-12 oxidase, CPR – cytochrome P450 reductase, DBR2 - artemisinic aldehyde Δ 11
749 (13) reductase, ALDH1 - aldehyde dehydrogenase.

750 **Figure 4. Principal component analysis of UPLC-MS (A) and GC-MS (B) data from**
751 **different leaf types from Artemis and NCV varieties.**

752 Principal component analysis of 75 UPLC-MS identified peaks (A) and 202 GC-MS identified
753 metabolites (B). Leaf types, corresponding with Figure 2 are represented by symbols: circles –
754 leaf 1-5, triangles – leaf 11-13, crosshairs – oven-dried leaf. Two chemotypes represented by
755 colours green – Artemis and grey – NCV. PCA was performed on log-scaled data and mean-
756 centred data; dotted ellipse = Hotelling's 95% confidence interval.

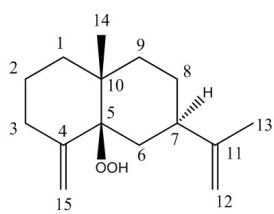
757 **Figure 5. Heatmaps of influential metabolites from UPLC- and GC-MS PCA analyses.**

758 Top-n (UPLC-MS = 18 (A); GC-MS = 20 (B)) metabolites were chosen for visualization based
759 on loadings plots (Supplementary Fig 1Y) from the PC1 dimensions in the PCA analyses (Fig
760 X). Mean data were log-scaled and then row-scaled for colour intensity plotting (lighter = more
761 abundant). Hierarchical clustering was performed with average linkage, with Euclidean distances
762 for genotypes and 1-absolute values of correlations as distances for metabolites. Metabolite
763 names are abbreviated where necessary for clarity and are given in full in Supplementary tables 2
764 and 3.

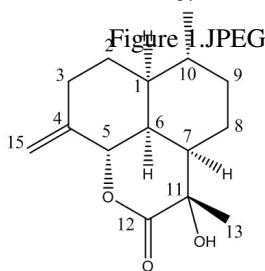
765 **Figure 6. Morphological characterisation of low- and high-artemisinin natural chemotypes**
766 **of *A. annua***

767 (A) Photographs show four representative 12-week old plants from each two chemotypes of *A.*
768 *annua*, ruler scaled in cm showed on both sides; Plant height (B), internode length (C), leaf area
769 (D) and glandular secretory trichome density (E) recorded for 12-week old plants. Green bars
770 represent Artemis (HAP-chemotype) and brown bars represent NCV (LAP-chemotype). Error
771 bars – SEM (n=15), letters represent one-way ANOVA Tukey's range test results; Groups not
772 sharing letters indicate statistically significant differences

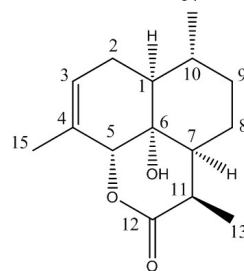
A



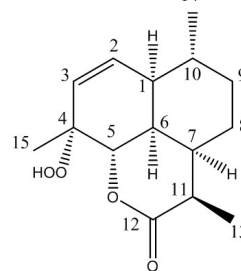
5 β -hydroperoxy-eudesma-4(15),11-diene (**4**)



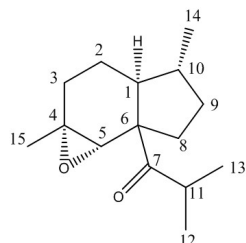
11-Hydroxy-arteanuin I (**18**)



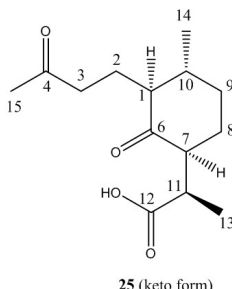
6 α -Hydroxy-arteanuin J (**19**)



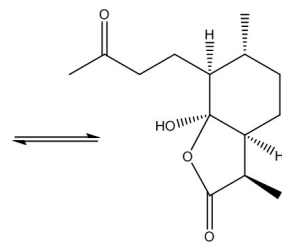
Arteannuin P (**20**)



abeo-Amorphane sesquiterpene (**27**)



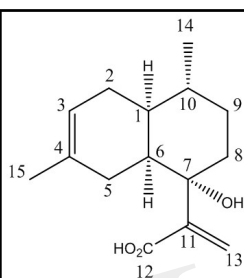
25 (keto form)



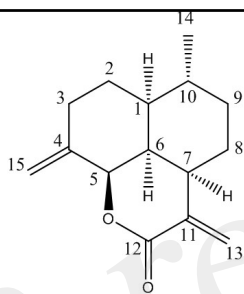
26 (ketal form)

Arteannuin Q (**25**)/(26)

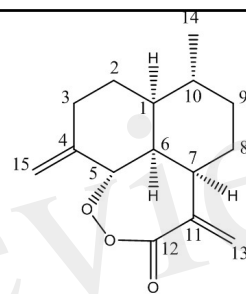
B



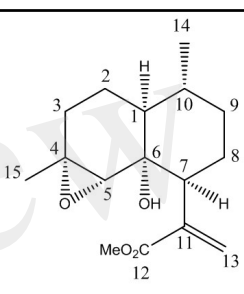
7 α -Hydroxy-isoartemisinic acid (**52**)



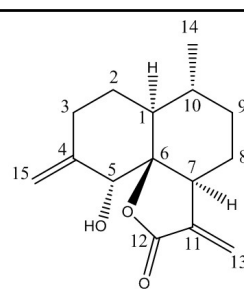
Arteannuin R (**54**)



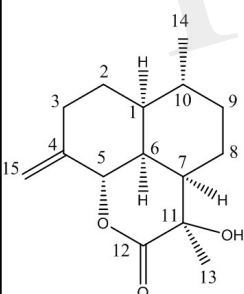
Arteannuin S (**55**)



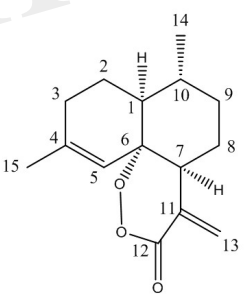
4 α , 5 α -Epoxy-6 α -hydroxyartemisinic acid methyl ester (**57**)



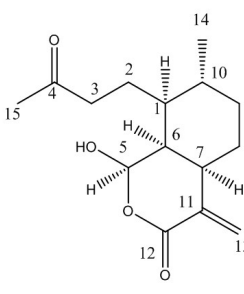
Dehydroarteanuin L (**59**)



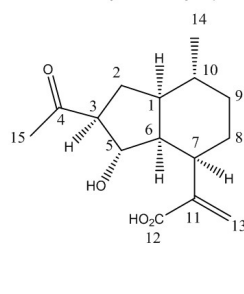
epi-11-Hydroxy-arteanuin I (**64**)



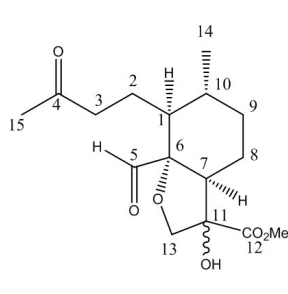
Artemisinic acid 6 α -peroxy ester (**65**)



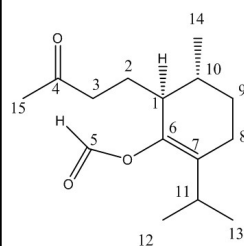
Arteannuin T (**69**)



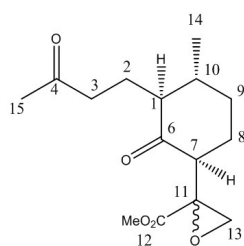
Arteannuin U (**70**)



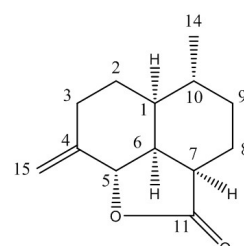
Arteannuin V (**72**)



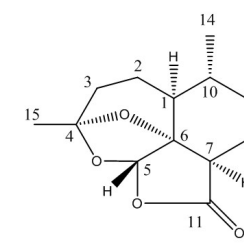
Arteannuin W (**73**)



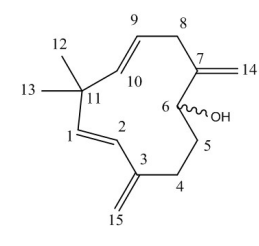
Arteannuin Y (**74**)



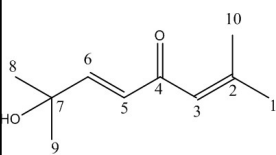
Isoarteanuin A (**77**)



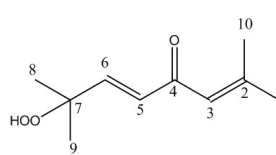
Arteannuin Z (**78**)



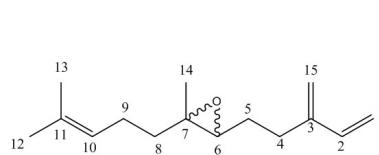
6-Hydroxy- γ -humulene (**48**)



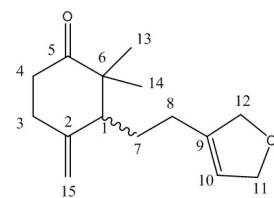
(*E*)-7-Hydroxy-2,7-dimethylocta-2,5-dien-4-one (**43**)



(*E*)-7-Hydroperoxy-2,7-dimethylocta-2,5-dien-4-one (**44**)

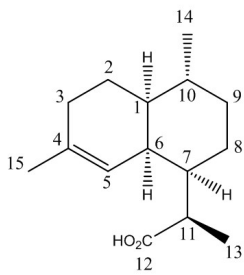


6,7-Epoxy-6,7-dihydro- β -farnesene (**45**)

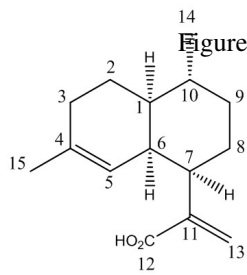


3-(2-(2,5-Dihydrofuran-3-yl)ethyl)-2,2-dimethyl-4-methylenecyclohexan-1-one (**79**)

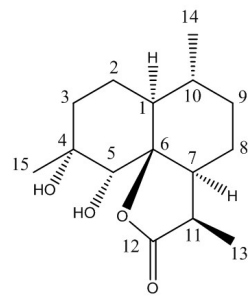
Figure 2.JPEG



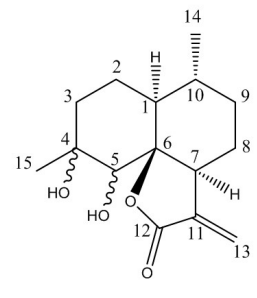
Dihydroartemisinic acid (8)



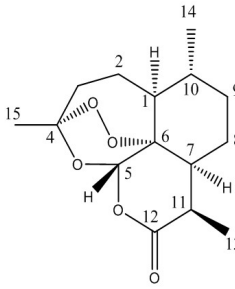
Artemisinic acid (9)



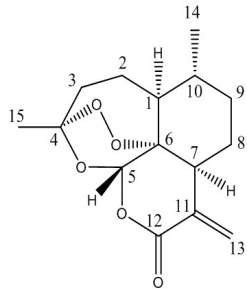
Arteannuin M (15)



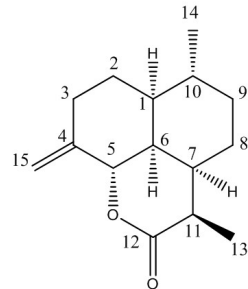
Dehydroarteannuin M (61)



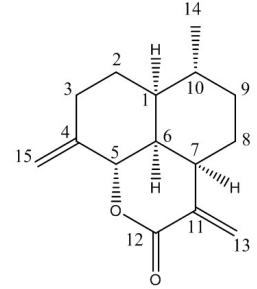
Artemisinin (22)



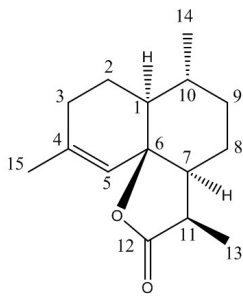
Artemisitene (66)



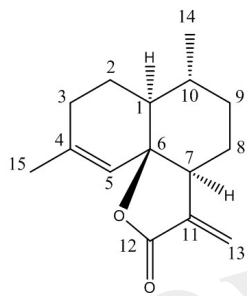
Arteannuin I (16)



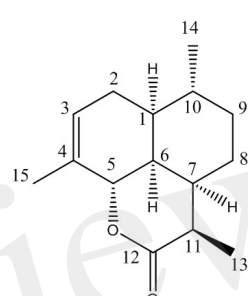
Annulide (62)



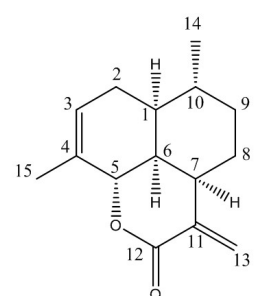
Dihydro-epi-deoxyarteannuin B (12)



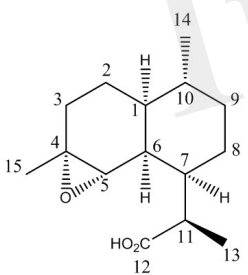
epi-Deoxyarteannuin B (13)



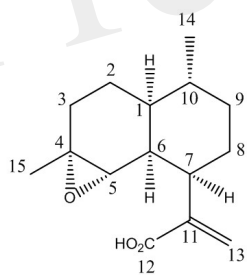
Arteannuin J (17)



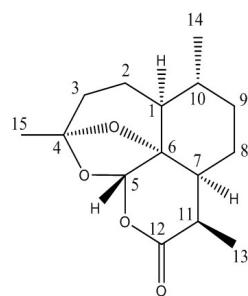
Isoannulide (63)



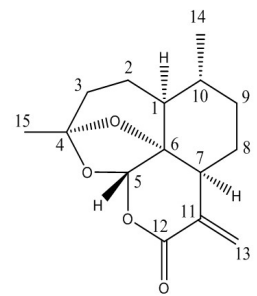
α -Epoxy-dihydroartemisinic acid (10)



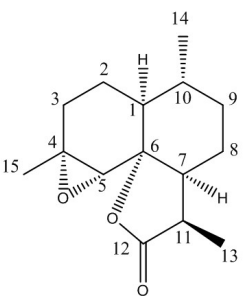
α -Epoxy-artemisinic acid (56)



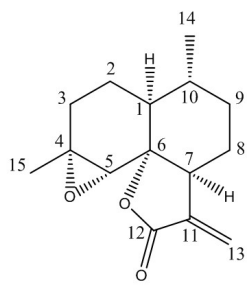
Deoxyartemisinin (23)



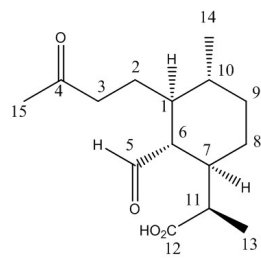
*Deoxyartemisitene (67)



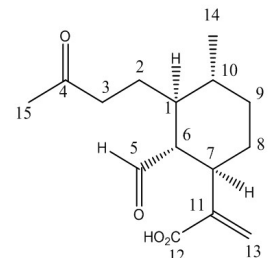
Dihydroarteannuin B (14)



Arteannuin B (60)



4,5-seco-4,5-Keto,aldehyde-amorphan-12-oic acid (24)



4,5-seco-4,5-Keto,aldehyde-amorphan-11,13-ene-12-oic acid (68)

Artemis

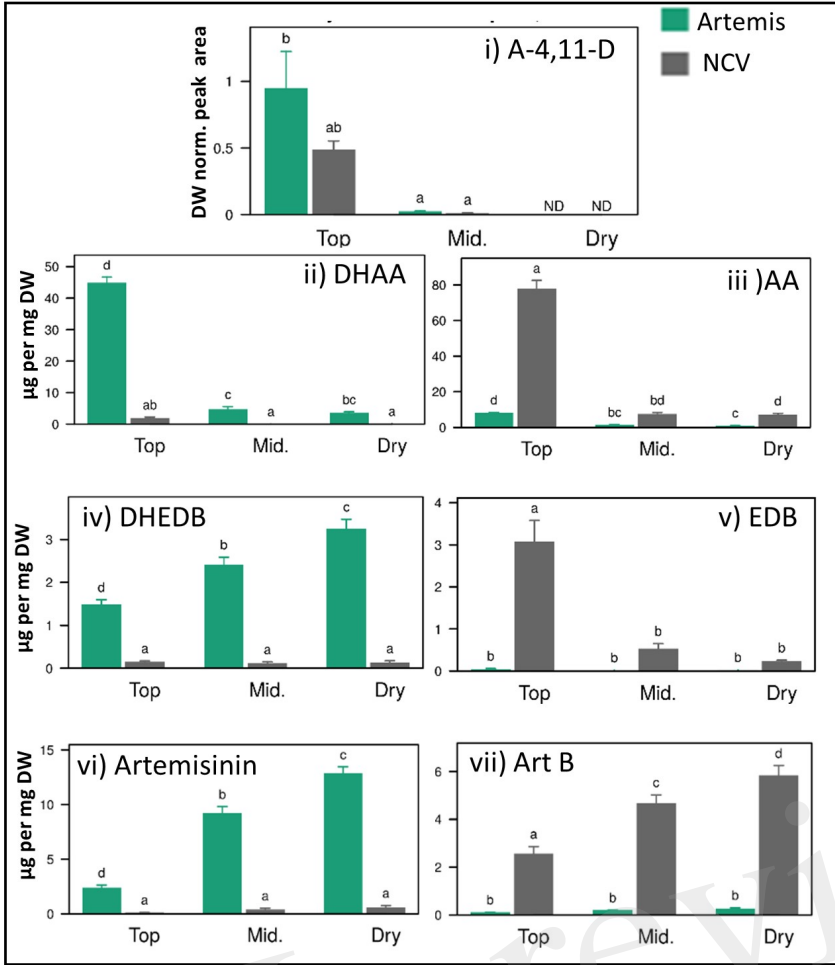
NCV

Artemis

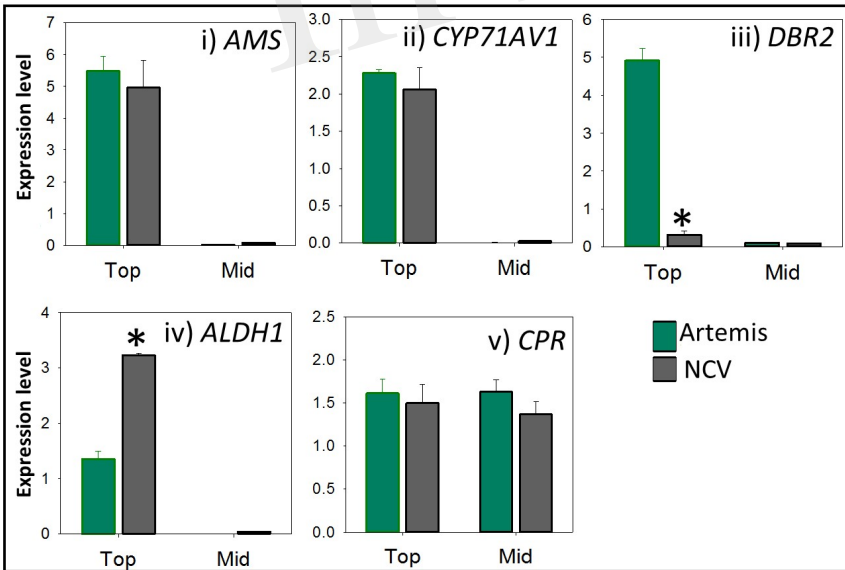
NCV

Figure 3.JPEG

A



B



C

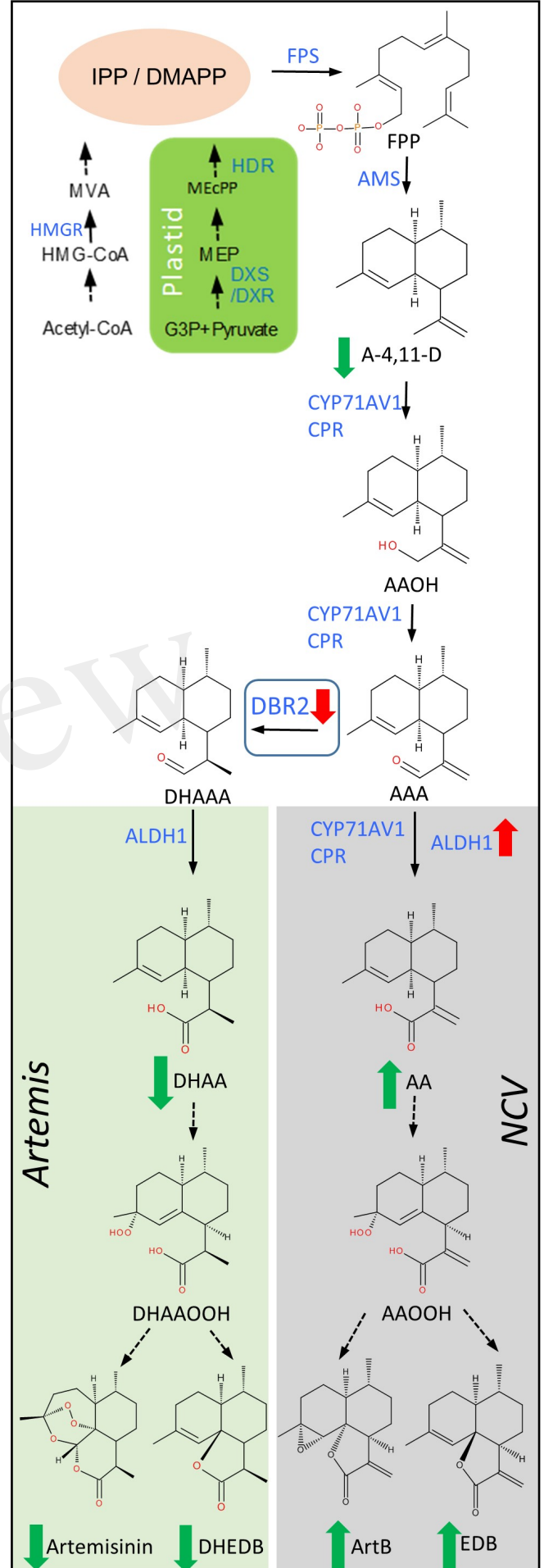


Figure 4.JPEG

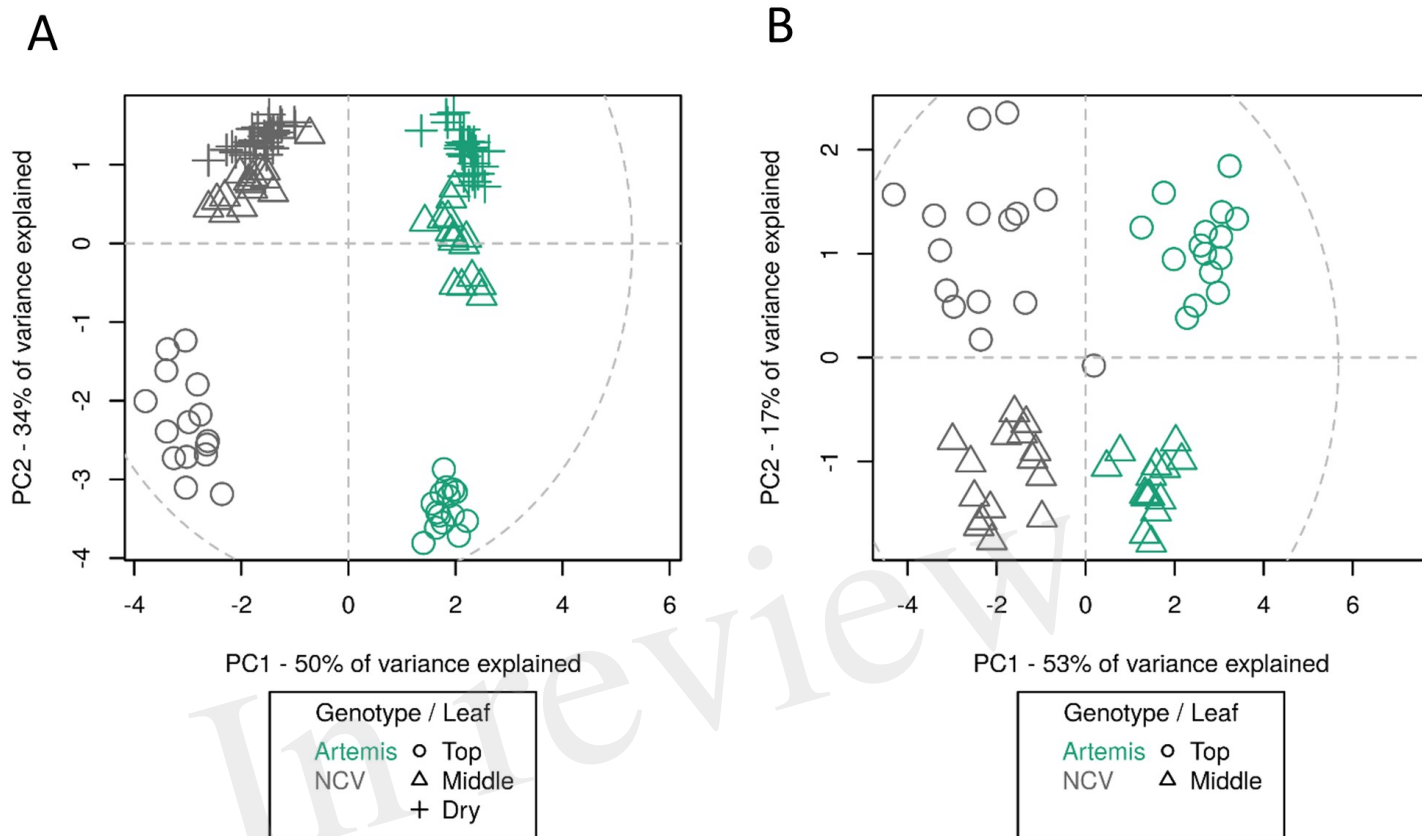


Figure 5.JPEG

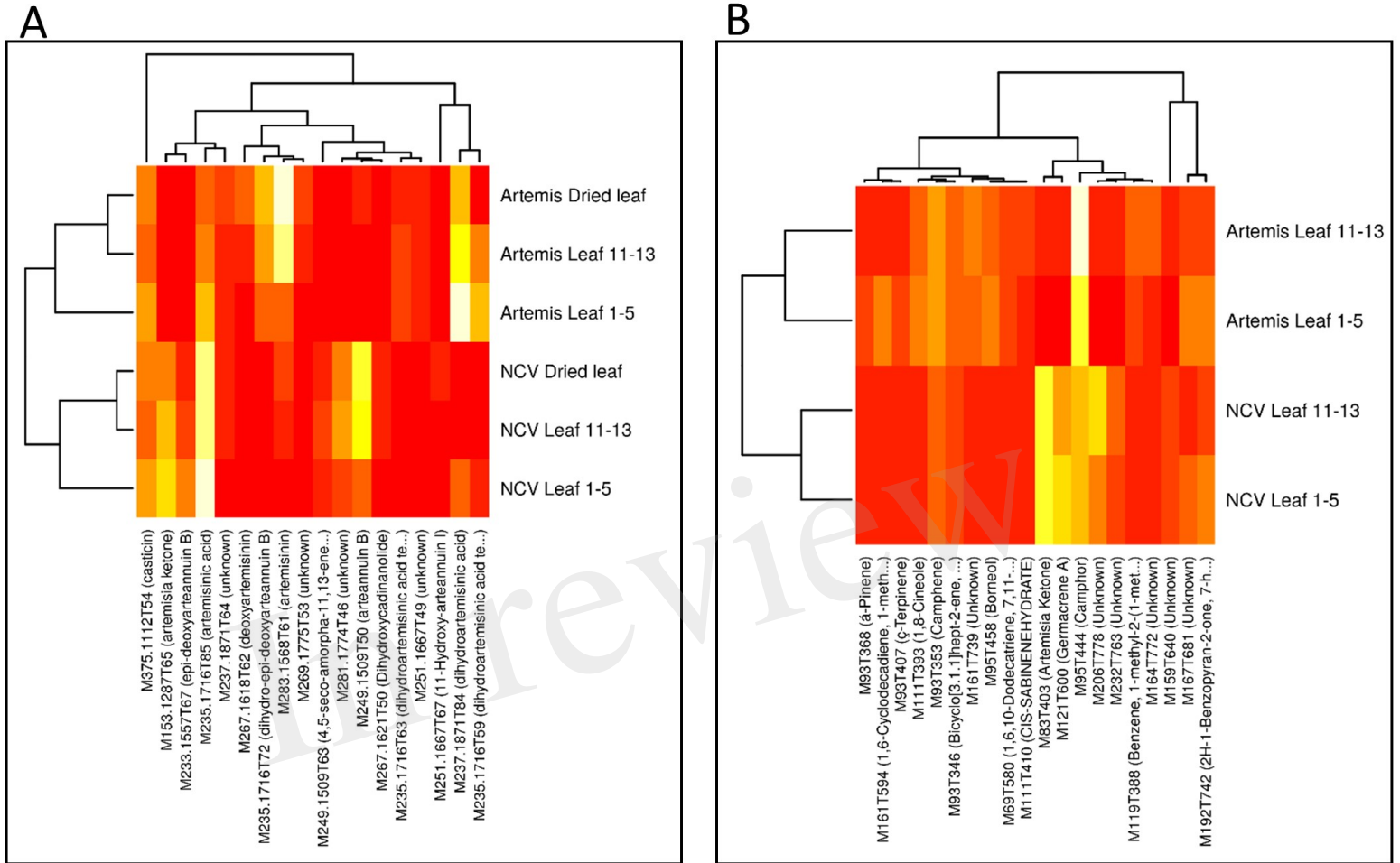
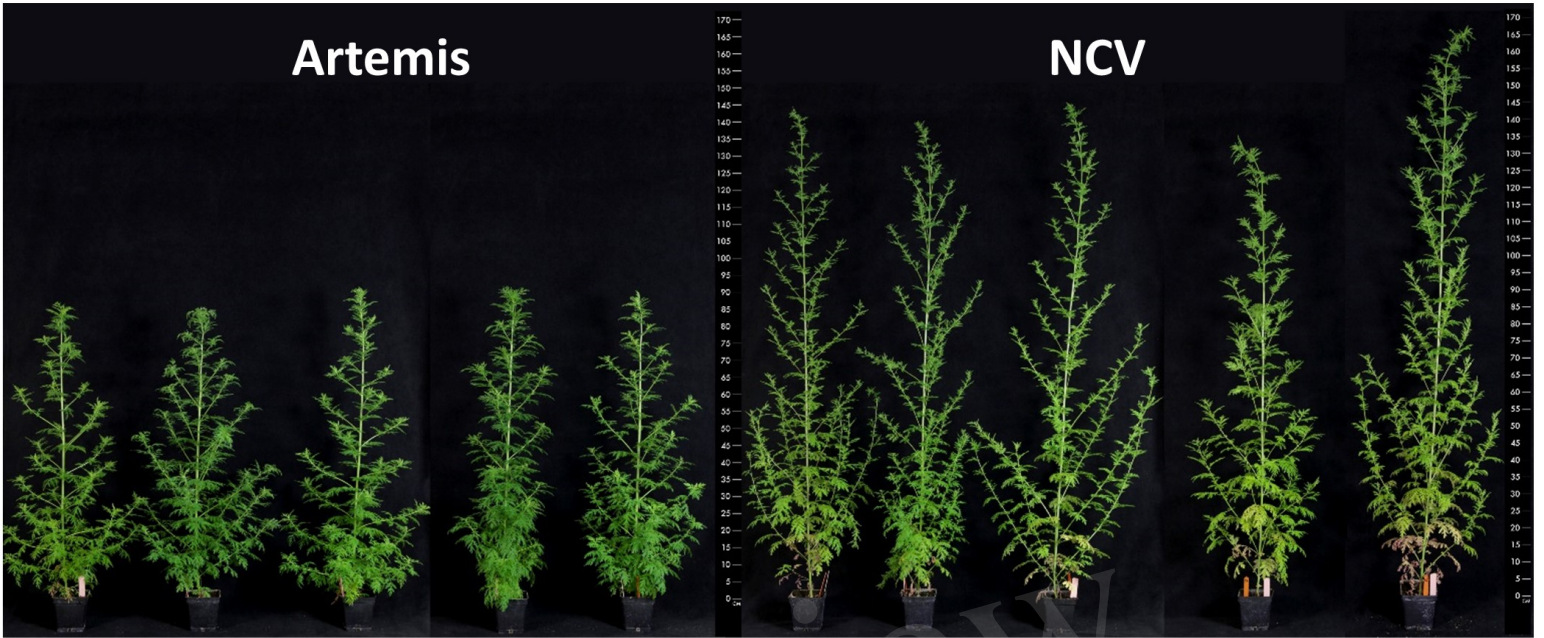
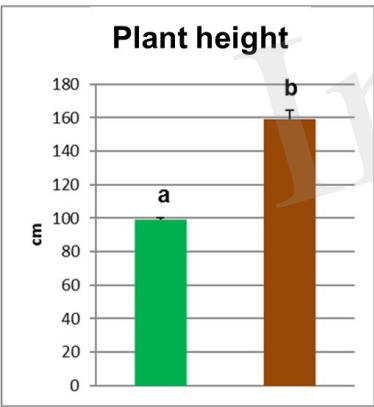


Figure 6.JPEG

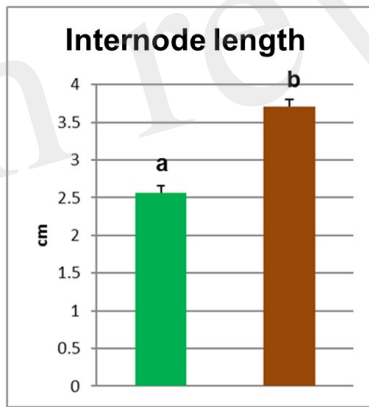
A



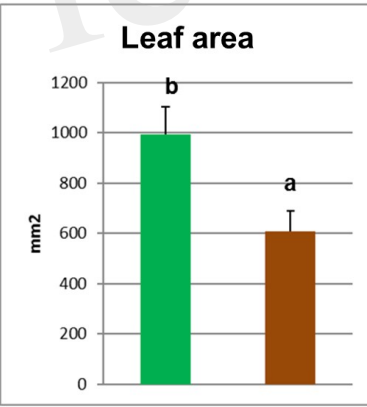
B



C



D



E

